CHAPTER

SIX

ELECTRICAL-RESISTANCE STRAIN GAGES

6.1 INTRODUCTION [1–4]

In the preceding chapter, several different strain-measuring systems were introduced, and their performance characteristics such as range, sensitivity, gage length, and precision of measurement were discussed. None of these different systems, regardless of the principle upon which the gage was based, exhibits all the properties required for an optimum device; however, the electrical-resistance strain gage approaches the requirements for an optimum system. As such, the electrical-resistance strain gage is the most frequently used device in stress-analysis work throughout the world today. Electrical-resistance strain gages are frequently used also as sensors in transducers designed to measure such quantities as load, torque, pressure, and acceleration.

The discovery of the principle upon which the electrical-resistance strain gage is based was made in 1856 by Lord Kelvin, who loaded copper and iron wires in tension and noted that their resistance increased with the strain applied to the wire. Furthermore, he observed that the iron wire showed a greater increase in resistance than the copper wire when they were both subjected to the same strain. Finally, Lord Kelvin employed a Wheatstone bridge to measure the resistance change. In this classic experiment he established three vital facts which have greatly aided the development of the electrical-resistance strain gage: (1) the resistance of the wire changes as a function of strain; (2) different materials have different sensitivities; and (3) the Wheatstone bridge can be used to measure these resistance changes accurately. It is indeed remarkable that over 80 years passed before strain gages based on Lord Kelvin's experiments became commercially available.

Today, after 40 years of commercial development and extensive utilization by industrial and academic laboratories throughout the world, the bonded-foil gage monitored with a Wheatstone bridge has become a highly perfected measuring system. Precise results for surface strains can be obtained quickly using relatively simple methods and inexpensive gages and instrumentation systems. In spite of the relative ease in employing strain gages, there are many features of the gages which must be thoroughly understood to obtain optimum performance from the measuring system in applied stress analysis. In this chapter, the electrical-resistance strain gage will be examined in detail to illustrate each feature affecting its performance. Strain-gage circuits and recording instruments used in measuring the strain-related resistance changes will be treated in Chaps. 8 and 9.

6.2 STRAIN SENSITIVITY IN METALLIC ALLOYS [5-8]

Lord Kelvin noted that the resistance of a wire increases with increasing strain and decreases with decreasing strain. The question then arises whether this change in resistance is due to the dimensional change in the wire under strain or to the change in resistivity of the wire with strain. It is possible to answer this question by performing a very simple analysis and comparing the results with experimental data which have been compiled on the characteristics of certain metallic alloys. The analysis proceeds in the following manner.

The resistance R of a uniform conductor with a length L, cross-sectional area A, and specific resistance ρ is given by

$$R = \rho \frac{L}{A} \tag{6.1}$$

Differentiating Eq. (6.1) and dividing by the total resistance R leads to

$$\frac{dR}{R} = \frac{d\rho}{\rho} + \frac{dL}{L} - \frac{dA}{A} \tag{a}$$

The term dA represents the change in cross-sectional area of the conductor due to the transverse strain, which is equal to $-\nu\, dL/L$. If the diameter of the conductor before the application of the axial strain is noted as d_0, then the diameter after the strain is applied is given by

$$d_f = d_0\left(1 - \nu \frac{dL}{L}\right) \tag{b}$$

and from Eq. (*b*) it is clear that

$$\frac{dA}{A} = -2\nu \frac{dL}{L} + \nu^2\left(\frac{dL}{L}\right)^2 \approx -2\nu \frac{dL}{L} \tag{c}$$

Substituting Eq. (*c*) into Eq. (*a*) gives

$$\frac{dR}{R} = \frac{d\rho}{\rho} + \frac{dL}{L}(1 + 2\nu)$$

which can be rewritten as

$$S_A = \frac{dR/R}{\epsilon} = 1 + 2\nu + \frac{d\rho/\rho}{\epsilon} \tag{6.2}$$

where S_A is the sensitivity of the metallic alloy used in the conductor and is defined as the resistance change per unit of initial resistance divided by the applied strain.

Examination of Eq. (6.2) shows that the strain sensitivity of any alloy is due to two factors, namely, the change in the dimensions of the conductor, as expressed by the $1 + 2\nu$ term, and the change in specific resistance, as represented by $(d\rho/\rho)/\epsilon$. Experimental results show that S_A varies from about 2 to 4 for most metallic alloys. For pure metals, the range is from -12.1 (nickel) to 6.1 (platinum). This fact implies that the change in specific resistance can be quite large for certain metals since $1 + 2\nu$ usually ranges between 1.4 and 1.7. Apparently, the change in specific resistance has its origin in variations in the number of free electrons and their mobility with applied strain.

A list of some metallic alloys commonly employed in commercial strain gages, together with their sensitivities, is presented in Table 6.1. It should be noted that the sensitivity depends upon the particular alloy being considered. Moreover, the values assigned to S_A in Table 6.1 are not necessarily constants. The value of the strain sensitivity S_A will depend upon the degree of cold working imparted to the conductor in its formation, the impurities in the alloy, and the range of strain over which the measurement of S_A is made.

Most electrical-resistance strain gages produced today are fabricated from the copper-nickel alloy known as Advance or Constantan. A typical curve showing the percent change in resistance $\Delta R/R$ as a function of strain for this alloy is given in Fig. 6.1. This alloy is useful in strain-gage applications for the following reasons:

1. The value of the strain sensitivity S_A is linear over a wide range of strain.

Table 6.1 Strain sensitivity S_A for common strain-gage alloys

Material	Composition, %	S_A
Advance or Constantan	45 Ni, 55 Cu	2.1
Nichrome V	80 Ni, 20 Cr	2.1
Isoelastic	36 Ni, 8 Cr, 0.5 Mo, 55.5 Fe	3.6
Karma	74 Ni, 20 Cr, 3 Al, 3 Fe	2.0
Armour D	70 Fe, 20 Cr, 10 Al	2.0
Platinum tungsten	92 Pt, 8 W	4.0

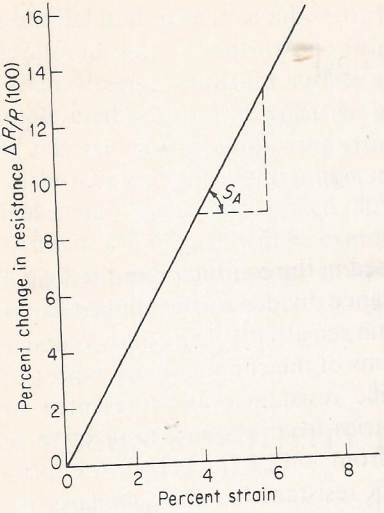

Figure 6.1 Percent change in resistance as a function of percent strain for an Advance alloy.

2. The value of S_A does not change as the material goes plastic.
3. The alloy has a high specific resistance ($\rho = 0.49\ \mu\Omega \cdot \text{m}$).
4. The alloy has excellent thermal stability and is not influenced appreciably by temperature changes when mounted on common structural materials.
5. The small temperature-induced changes in resistance of the alloy can be controlled with trace impurities or by heat treatment.

The first advantage of the Advance-type alloy over other alloys implies that the gage calibration constant will not vary with strain level; therefore, a single calibration constant is adequate for all levels of strain. The wide range of linearity with strain (even into the alloy's plastic region) indicates that it can be employed for measurements of both elastic and plastic strains in most structural materials. The high specific resistance of the alloy is useful when constructing a small gage with a relatively high resistance. Finally, the temperature characteristics of selected melts of the alloy permit the fabrication of temperature-compensating strain gages for each structural material. With temperature-compensated strain gages, the temperature-induced $\Delta R/R$ on a given material can be maintained at less than 10^{-6} per Celsius degree.

The Isoelastic alloy is also employed in commercial gages because of its high sensitivity (3.6 for Isoelastic compared with 2.1 for Advance) and its high fatigue strength. The increased sensitivity is advantageous in dynamic applications where the strain-gage output must be amplified to a considerable degree before recording. The high fatigue strength is useful when the gage is to operate in a cyclic strain field where the alternating strains exceed 1500 μin/in (μm/m). In spite of these two advantages, the Isoelastic alloy has two disadvantages which severely limit its use. First, this alloy is extremely sensitive to temperature changes; and when it is mounted in gage form on a steel specimen, a change in temperature of 1°C will

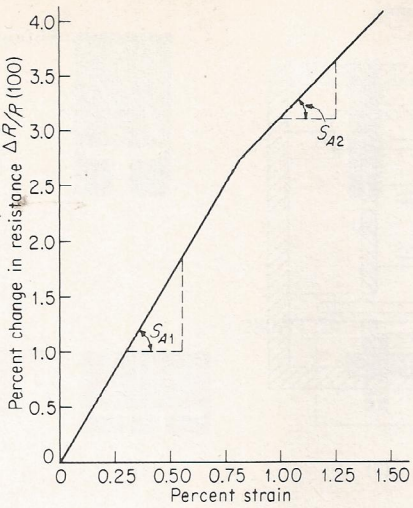

Figure 6.2 Percent change in resistance as a function of percent strain for an Isoelastic alloy.

give an apparent strain indication of 300 to 400 μin/in (μm/m). It can be used in dynamic applications only when the temperature is stable over the time required for the dynamic measurement. A second disadvantage of the Isoelastic alloy is its limited linearity, as illustrated in Fig. 6.2. At a strain level of approximately 0.75 percent, the sensitivity S_A of the alloy changes from approximately 3.6 to 2.5. This fact implies that for strains greater than 7,500 μin/in (μm/m) the calibration factor associated with the gage must be changed to correspond with the reduction in S_A from 3.6 to 2.5.

The Karma alloy is used in temperature-compensated gages in the same manner as the Advance alloy. The range of temperature over which compensation can be achieved, however, is larger for Karma than for Advance. Also, the Karma alloy has a higher resistance to cyclic strain than the Advance alloy.

The other alloys, Nichrome V, Armour D, and the platinum-tungsten alloy, are used for special-purpose gages which permit measurements of strain to be made at temperatures in excess of 450°F (230°C).

6.3 GAGE CONSTRUCTION [9–14]

It is theoretically possible to measure strain with a single length of wire as the sensing element of the strain gage; however, circuit requirements needed to prevent overloading of the power supply and to minimize heat generated by the gage current place a lower limit of approximately 100 Ω on the gage resistance. As a result, a 100-Ω strain gage fabricated from wire having a diameter of 0.001 in (0.025 mm) and a resistance of 25 Ω/in (1000 Ω/m) requires a single length of wire 4 in (100 mm) long.

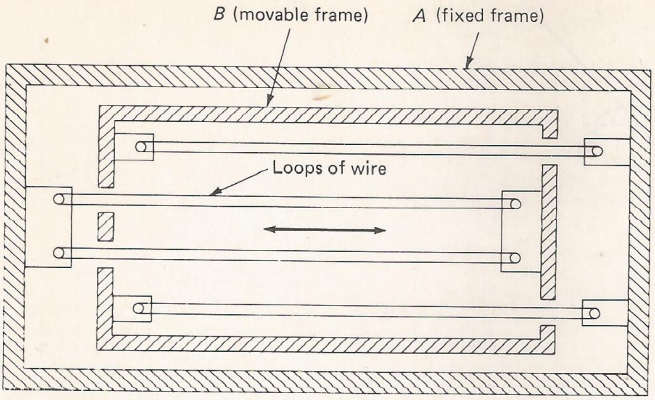

Figure 6.3 An unbounded-wire strain gage.

The very earliest electrical-resistance strain gages were of the unbonded type, where the conductors were straight wires strung between a movable frame and a fixed frame as shown in Fig. 6.3. This gage was large and required knife-edges for mounting, which greatly limited its applicability.

The problem of conductor length and gage mounting was solved in the mid-1930s, when Ruge and Simmons independently developed bonded-wire strain gages. The conductor-length problem was solved by forming the required length of wire into a grid pattern. The attachment problem was solved by bonding the wire grid directly to the specimen with suitable adhesives. Wire gages were produced with both flat-grid and bobbin-type constructions, as illustrated in Fig. 6.4. Bonded-wire strain gages were employed for strain measurements almost

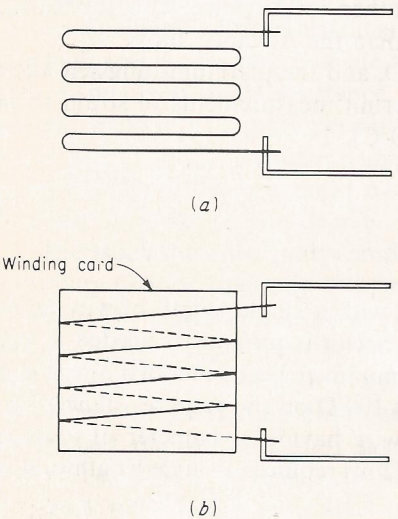

Figure 6.4 (*a*) Flat-grid and (*b*) bobbin-type constructions for bonded-wire-type resistance strain gages.

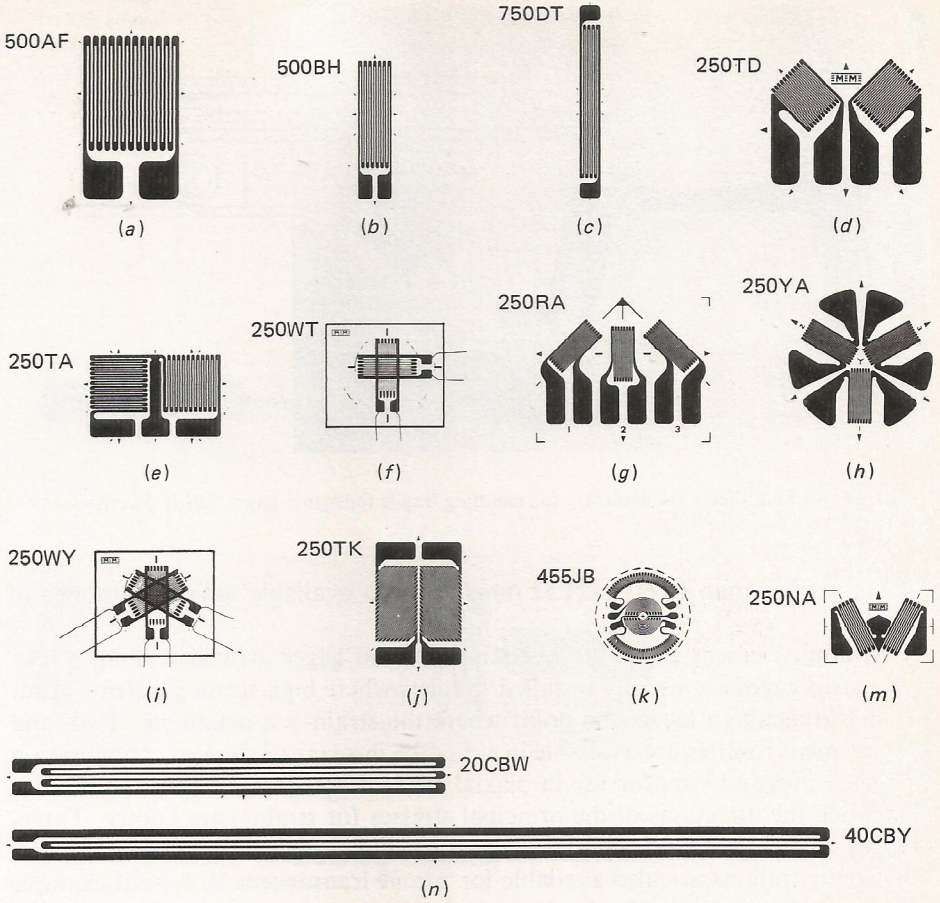

Figure 6.5 Configurations of metal-foil strain gages: (*a*) single-element gage, (*b*) single-element gage, (*c*) single-element gage, (*d*) two-element rosette, (*e*) two-element rosette, (*f*) two-element stacked rosette, (*g*) three-element rosette, (*h*) three-element rosette, (*i*) three-element stacked rosette, (*j*) torque gage, (*k*) diaphragm gage, (*m*) stress gage, (*n*) single-element gage for use on concrete. (*Micro-Measurements.*)

exclusively, from the mid-1930s to the mid-1950s. They are still used occasionally today, but in most instances they have been replaced by the bonded-foil strain gage.

The first metal-foil strain gages were produced in England in 1952 by Saunders and Roe. With this type of gage, the grid configuration is formed from metal foil by a photoetching process. Since the process is quite versatile, a wide variety of gage sizes and grid shapes can be produced. Typical examples of the variety of gages marketed commercially are illustrated in Fig. 6.5. The shortest gage length available in a metal-foil gage is 0.008 in (0.20 mm). The longest gage length is 4.00 in (102 mm). Standard gage resistances are 120 and 350 Ω. Gages having

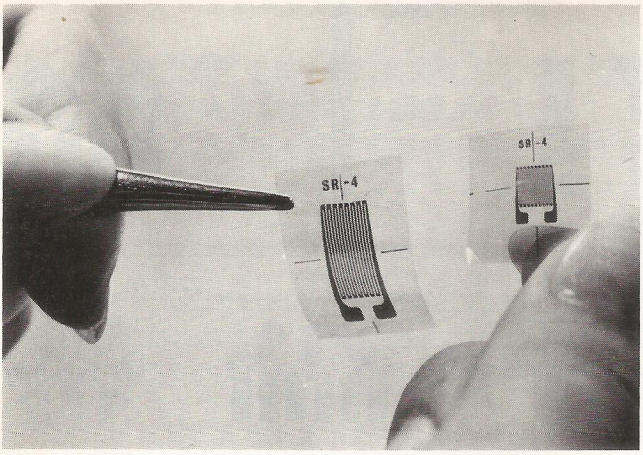

Figure 6.6 Backing sheets are necessary for handling fragile foil strain gages. (*BLH Electronics.*)

lengths greater than 0.060 in (1.52 mm) are also available with a resistance of 1000 Ω.

Multiple-element gages are available with 10 gages arranged along a line. These strip gages are usually installed in fillets where high strain gradients occur and it is difficult to locate the point where the strain is a maximum. Two- and three-element rosettes are available in either the in-plane or stacked configuration in a wide range of sizes for use in biaxial stress fields. Two-element rosettes are used when the directions of the principal stresses (or strains) are known. Three-element rosettes are used when the principal directions are not known. Special gage configurations are also available for use in transducers. A typical example is shown in Fig. 5.6*k* for the diaphragm-type pressure transducer.

The etched metal-film grids are very fragile and easy to distort, wrinkle, or tear. For this reason, the metal film is usually bonded to a thin plastic sheet, which serves as a backing or carrier before photoetching. The carrier material also provides electrical insulation between the gage and the component after the gage is mounted. The use of a backing sheet to serve as a carrier for the grid is illustrated in Fig. 6.6, which shows a gage being handled. Markings for the centerline of the gage length and width are also displayed on the carrier.

Very thin paper was the first carrier material employed in the production of wire-type gages, and its use has been maintained to a limited extent. More recently, a thin (0.001-in, or 0.025-mm) sheet of polyimide, which is a tough and flexible plastic, has been used as a carrier for strain gages intended for general-purpose stress analysis. For transducer applications, where precision and linearity are very important, a very thin high-modulus epoxy is used for the carrier. The epoxy backing is not suitable for general-purpose strain gages since it is brittle and can easily be broken during gage installation. Glass-fiber-reinforced epoxy and/or phenolics are employed as carriers when the strain gage will be exposed to high-

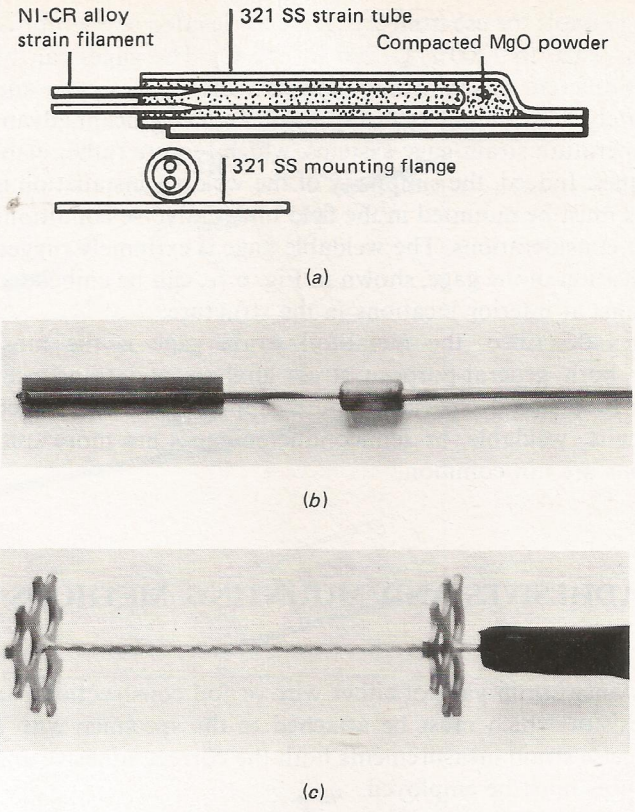

Figure 6.7 Weldable strain gages: (*a*) construction details, (*b*) external appearance of a gage, (*c*) gage for embedment in concrete. (*Ailtech.*)

level cyclic strains and fatigue life of the gage system is important. In this application, the carrier is used to encapsulate the grid. Glass-reinforced epoxy carriers are also used for moderate temperature applications up to 750°F (400°C). For very high temperature applications, a strippable carrier is used. This carrier is removed during application of the gage, and a ceramic adhesive serves to maintain the grid configuration and to insulate the gage.

Another type of gage, originally developed for high-temperature strain measurement, is the weldable strain gage (Fig. 6.7). It consists of a very fine loop of wire which is swaged into a metal case with compacted MgO powder as an insulator. The wire ends are connected to integral lead wires in a metal case. The wire inside the strain tube is reduced in diameter by an etching process; hence, the minimum gage resistance is obtained with a very-small-diameter, high-resistance wire rather than by forming a grid of larger-diameter wire.

Currently the weldable gages are available with resistances which range from 60 to 350 Ω and with lengths which range from 0.375 in (9.5 mm) to 1.09 in

(27.7 mm). The gages are suitable for use from cryogenic to elevated temperatures or within the range from −320 to 1200°F (−200 to 650°C). The gages can be welded onto a number of different metals with a capacitor discharge welder and are ready for use immediately. This simplicity in application is a significant advantage over other high-temperature strain-gage systems, which require rather elaborate installation techniques. Indeed, the simplicity of the welding installation is attractive whenever gages must be mounted in the field under adverse conditions regardless of temperature considerations. The weldable gage is extremely rugged and waterproof. A modification of the gage, shown in Fig. 6.7*c*, can be embedded in concrete to record strains at interior locations in the structure.

Of the various gages described, the metal-foil strain gage is the most frequently employed for both general-purpose stress analysis and transducer applications. There are occasional special-purpose applications for which unbonded-wire, bonded-wire, weldable, or semiconductor gages are more suitable, but these applications are not common.

6.4 STRAIN-GAGE ADHESIVES AND MOUNTING METHODS [15–21]

The bonded type of resistance strain gage of either wire or foil construction is a high-quality precision resistor which must be attached to the specimen with a suitable adhesive. For precise strain measurements both the correct adhesive and proper mounting procedures must be employed.

The adhesive serves a vital function in the strain-measuring system; it must transmit the strain from the specimen to the gage sensing element without distortion. It may appear that this role can be easily accomplished if the adhesive is suitably strong; however, the characteristics of the polymeric adhesives used to bond strain gages are such that, as will be shown later, the adhesive can influence apparent gage factor, hysteresis characteristics, resistance to stress relaxation, gage resistance, temperature-induced zero drift, and insulation resistance.

The singularly unimpressive feat of bonding a strain gage to a specimen is perhaps one of the most critical steps in the entire process of measuring strain with a bonded resistance strain gage. The improper use of an adhesive costing a few dollars per test can seriously degrade the validity of an experimental stress analysis which may cost thousands of dollars.

When mounting a strain gage, it is important to carefully prepare the surface of the component where the gage is to be located. This preparation consists of sanding away any paint or rust to obtain a smooth but not highly polished surface. Next, solvents are employed to remove all traces of oil or grease. Finally, the clean, sanded, and degreased surface is treated with a basic solution to give the surface the proper chemical affinity for the adhesive.

The gage location is then marked on the specimen and the gage is positioned by using a rigid transparent tape in the manner illustrated in Fig. 6.8. The position

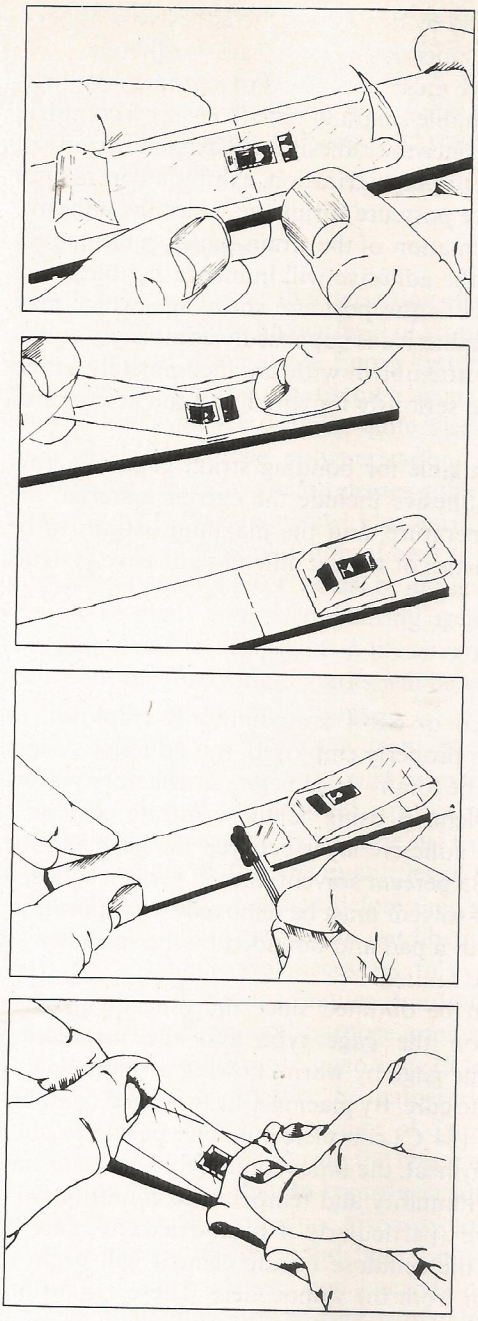

Figure 6.8 The tape method of installation for metal-foil strain gages. (*Micro-Measurements.*)

and orientation of the gage are maintained by the tape as the adhesive is applied and as the gage is pressed into place by squeezing out the excess adhesive.

After the gage is installed, the adhesive must be exposed to a proper combination of pressure and temperature for a suitable length of time to ensure a complete cure. This curing process is quite critical since the adhesive will expand because of heat, experience a volume reduction due to polymerization, exhibit a contraction upon cooling, and on occasion experience postcure shrinkage. Since the adhesive is sufficiently strong to control the deformation of the strain-sensitive element in the gage, any residual stresses set up in the adhesive will influence the output of the strain gage. Of particular importance is the postcure shrinkage, which may influence the gage output long after the adhesive is supposedly completely cured. If a long-term strain measurement is attempted with an incompletely cured adhesive, the stability of the gage will be seriously impaired and the accuracy of the measurements compromised.

A wide variety of adhesives are available for bonding strain gages. Factors influencing the selection of a specific adhesive include the carrier material, the operating temperature, the curing temperature, and the maximum strain to be measured. A discussion of the characteristics of several different adhesive systems in common use follows.

A. Cellulose Nitrate Cement

Cellulose nitrate cements such as Duco or SR-4 are commonly employed to mount paper-backed strain gages. When properly employed, this adhesive system is adequate; however, the adhesive must be totally dried before satisfactory performance is obtained. The primary problem in using cellulose nitrate cement is assisting the solvent to escape from the adhesive layer between the gage and the specimen. Since the cement consists of 85 percent solvent and 15 percent solids, it is evident that an appreciable amount of solvent must be removed by evaporation. Moreover, the gage is often covered with a pad and bounded by the specimen so that the passages for solvent release are limited.

No standard curing procedure can be outlined since the time involved in evaporating the solvent depends upon the gage type and the installation procedure. However, heat applied to the gage by warm, flowing air appreciably shortens the time required for a complete cure. By placing a strain-gaged component in an air-circulating oven at 130°F (54°C) complete cure can be effected in a day or two. If it is not possible to employ heat, the time required for complete cure is greatly extended and depends upon humidity and temperature conditions.

Once the gage is completely dried (particularly if oven-dried), it must be waterproofed immediately. Otherwise the cellulose nitrate cement will begin to expand as a result of water absorption from the atmosphere. These expansions occur slowly since they are diffusion-induced; nevertheless, if the readout period is long, the expansion of the cement can materially influence the gage reading and create instabilities and generally unsatisfactory performance of the measuring system.

Perhaps the best indication of a properly cured adhesive system can be obtained by measuring the resistance between the gage grid and the specimen (resistance through the adhesive layer). A properly dried installation will exhibit a resistance to ground exceeding 10,000 MΩ. Minute traces of either solvent or water in the adhesive will lower the resistance of the adhesive layer and influence gage performance.

B. Epoxy Cements

Epoxies are a class of thermosetting plastics which, in general, exhibit a higher bond strength and a higher level of strain at failure than other types of adhesives used to mount strain gages. Epoxy systems are usually composed of two constituents, a monomer and a hardening agent. The monomer, or base epoxy, is a light amber fluid which is usually quite viscous. A hardening agent mixed with the monomer will induce polymerization. Amine-type curing agents produce an exothermic reaction which releases sufficient heat to accomplish curing at room temperature or at relatively low curing temperatures. Anhydride-type curing agents require the application of heat to promote polymerization. Temperatures in excess of 250°F (120°C) must be applied for several hours to complete polymerization. So many epoxies and curing agents are commercially available today that it is impossible to be specific in the coverage of their properties or their behavior. However, the following remarks will be valid and useful for any system of epoxies used in strain-gage applications.

With both types of curing agent, particularly the amine type, the amount of hardener added to the monomer is extremely important. The adhesive curing temperatures and the residual stresses produced during polymerization can be significantly influenced by as little as 1 or 2 percent variance from the specified values. For this reason, the quantities of both the monomer and the curing agent should be carefully weighed before they are mixed together.

In general, pure epoxies do not liberate volatiles during cure; therefore, post-cure heat cycling is not necessary to evaporate chemical by-products released during polymerization. Volatiles should not be added to the epoxies to improve their viscosity for general-purpose applications. A filler material such as Cabosil can be added in moderate quantities (5 to 10 percent by weight) to improve the bond strength and to reduce the temperature coefficient of expansion of the epoxy.

A modest clamping pressure of 5 to 20 lb/in^2 (35 to 140 kPa) is recommended for the epoxies during the cure period to ensure as thin a bond line (adhesive layer) as possible. In transducer applications, solvent-thinned epoxies are frequently specified to reduce viscosity so that extremely thin (less than 200 μin, or 0.005 mm) void-free bond lines can be obtained. Thin bond lines tend to minimize creep, hysteresis, and linearity problems. For these transducer applications, clamping pressures of approximately 50 lb/in^2 (350 kPa) are recommended.

Many different epoxy systems are available from strain-gage manufacturers in kit form with the components preweighed. These systems are recommended since the epoxies are especially formulated for strain-gage applications. They are easy

and convenient to use, they have an adequate pot life, and the time-temperature curve for the curing cycle is specified. The use of hardware-store variety two-tube epoxy systems is discouraged since these systems usually incorporate modifiers or plasticizers which although they improve the toughness of the adhesive cause large amounts of creep and hysteresis undesirable for strain-gage applications.

C. Cyanoacrylate Cement (Eastman 910 SL)

A modified form of Eastman 910 adhesive consisting of a methyl-2-cyanoacrylate compound is commonly employed as a strain-gage adhesive. This adhesive system is simple to use, and the strain gage can be employed approximately 10 min after bonding. Chemically, this adhesive is quite unusual in that it requires neither heat nor catalyst to induce polymerization. Apparently when this adhesive is spread in a thin film between two components to be bonded, the minute traces of water or other weak bases on the surfaces of the components are sufficient to trigger the polymerization process. A catalyst can be applied to the bonding surfaces to decrease the reaction times, but it is not essential.

In strain-gage applications, a thin film of the adhesive is placed between the gage and the specimen and a gentle pressure is applied for about 1 or 2 min to induce polymerization. Once initiated, the polymerization will continue at room temperature without the pressure required initially.

The fast room-temperature cure of the cyanoacrylate adhesive makes it ideal for general-purpose strain-gage applications. The performance of this adhesive system, however, will deteriorate with time, moisture absorption, or elevated temperature; therefore, it should not be used where extended life of the gage system is important. Coatings such as microcrystalline wax, silicone rubber, polyurethane, etc., can be used to protect the adhesive from moisture in the air and extend the life of an installation to 1 or 2 years.

D. Ceramic Cements

Two different approaches are used in bonding strain gages with ceramic adhesives. The first utilizes a blend of finely ground ceramic powders such as alumina and silica combined with a phosphoric acid. Usually this blend of powders is mixed with a solvent such as isopropyl alcohol and an organic binder to form a liquid mixture which facilitates handling. A precoat of the ceramic cement is applied and fired to form a thin layer of insulation between the gage grid and the component. A second layer of ceramic cement is then applied to bond the gage. In this application, the carrier for the gage is removed, and the grid is totally encased in ceramic.

Since many of the ceramic cements marketed commercially have proprietary compositions, it is often difficult to select the most suitable product. One cement, developed by the National Bureau of Standards and identified as NBS-x-142, is recommended for high-temperature use since it exhibits a very high resistivity at temperatures up to 1800°F (980°C). Gage resistance to ground with this cement

Table 6.2 Composition of NBS-x-142 ceramic cement

Constituent	Parts by weight
Alumina, Al_2O_3	100
Silica, SiO_2	100
Chrome anhydride, CrO_3	2.5
Colloidal silica solution	200
Orthophosphoric acid, H_3PO_4	30

will normally exceed 6 MΩ. The composition of the NBS-x-142 cement is given in Table 6.2. The ceramic cements are used primarily for high-temperature applications or in radiation environments, where organic adhesives cannot be employed.

A second method for bonding strain gages with a ceramic material utilizes a flame-spraying Rokide process. A special gun (Fig. 6.9) is used to apply the ceramic particles to the gage. For this type of application, gages of wire construction

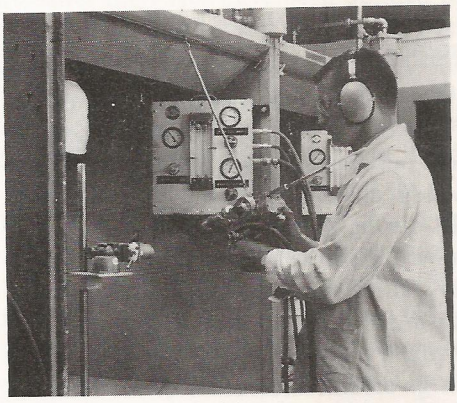

(*a*)

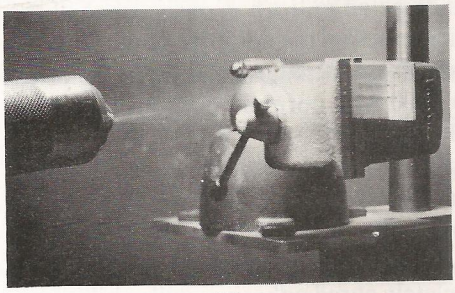

(*b*)

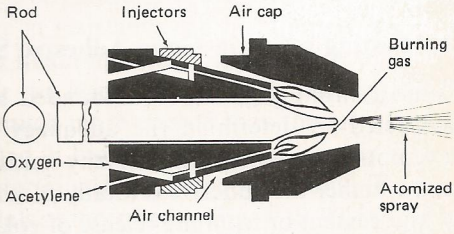

(*c*)

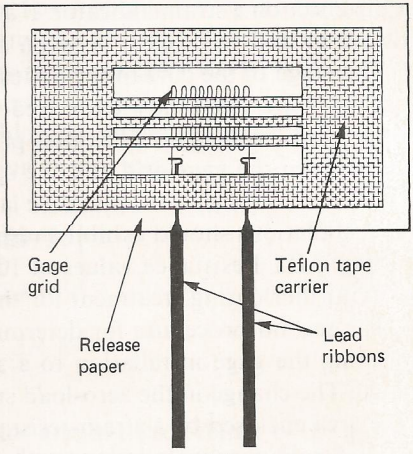

(*d*)

Figure 6.9 Flame spraying ceramic adhesives: (*a*) flame-spray gun in operation, (*b*) strain gage with carrier on a specimen, (*c*) particle formation in the spray gun, (*d*) free element strain gage with carrier. (*BLH Electronics.*)

mounted on slotted carriers are used. The carrier, which holds the gage and lead wires in position during attachment, is made from a glass-reinforced Teflon tape. The tape is resistant to the molten flame-sprayed ceramic particles; however, after the gage grid is secured to the component, the tape is removed and the grid is completely encased with flame-sprayed ceramic particles.

The flame-spray gun utilizes an oxyacetylene gas mixture in a combustion chamber to produce very high temperatures. Ceramic material in rod form is fed into the combustion chamber; there the rod decomposes into softened semimelted particles which are forced from the chamber by the burning oxyacetylene gas. The particles impinge on the surface of the component and form a continuous coating. Since the particles (even in their softened state) are somewhat abrasive, foil grids are not normally used.

Most gage installations are made with BLH-H rod, which is essentially pure alumina, or with BLH-S rod, which is alumina with about 2 percent silica. For applications involving temperatures less than 800°F (425°C), the S rod is employed since it is easier to melt and apply. The H rod is intended for higher-temperature applications.

E. Testing a Strain-Gage Adhesive System

After a strain gage has been bonded to the surface of a specimen, it must be inspected to determine the adequacy of the bond. The inspection procedure attempts to establish whether any voids exist between the gage and the specimen and whether the adhesive is totally cured. Voids can result from bubbles originally in the cement or from the release of volatiles during the curing process. They can be detected by tapping the gage installation with a soft rubber eraser and observing the effect on a strain indicator. If a strain reading is noted, the gage bond is not satisfactory and voids exist between the sensing element and the specimen.

The stage of the cure of the adhesive is much more difficult to establish. Two procedures are frequently employed which give some indication of the relative completeness of the cure. The first procedure utilizes measurement of the resistance between the gage grid and the specimen as an indication of the stage of the cure. The resistance of the adhesive layer increases as the adhesive cures. Typical gage installations should exhibit a resistance across the adhesive layer of the order of 10,000 MΩ. Resistance values of 100 to 1000 MΩ normally indicate a need to specify further curing treatment for the adhesive.

The second procedure for determining the completeness of the cure involves subjecting the gage installation to a strain cycle while measuring the resistance change. The change in the zero-load strain reading after a strain cycle (zero shift) or the area enclosed by a strain-resistance change curve is a measure of the degree of cure. Strain-gage installations with completely cured adhesives will exhibit zero shifts of less than 2 μin/in (μm/m) of apparent strain. Should larger values of zero shift be observed, the adhesive should be subjected to a postcure temperature cycle.

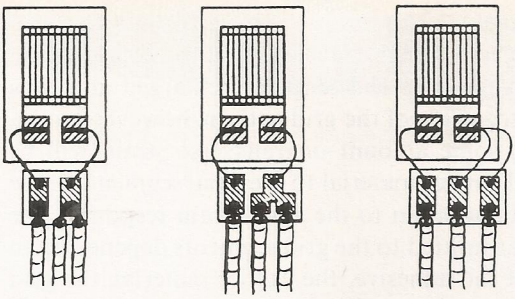

Figure 6.10 Use of anchor terminals to connect lead wires to gages. (*Micro-Measurements.*)

In the event that the gages are mounted on a component or a structure which cannot be strain-cycled before testing, a temperature cycle can be substituted for the strain cycle. If the adhesive in a gage installation has been thoroughly cured, no change in the zero strain will be observed when the gage is returned to its original temperature. If the adhesive cure is incomplete, the temperature cycle will result in additional polymerization with associated shrinkage of the adhesive which causes a shift in the zero reading of the gage.

After the gages have been bonded to the structure or component, it is necessary to attach lead wires so that the change in resistance can be monitored on a suitable instrumentation system. Since the metal-foil strain gages are relatively fragile, care must be exercised in attaching the lead wires to the soldering tabs. Intermediate anchor terminals, which are much more rugged than the metal-foil gage tabs, are usually employed, as illustrated in Fig. 6.10. A small-diameter wire (32- to 36-gage) is used to connect the gage terminal to the anchor terminal. Three lead wires are soldered to the anchor terminals as indicated in Fig. 6.10. The use of three lead wires to ensure temperature compensation in the Wheatstone bridge measuring circuit will be discussed in Sec. 8.6. The size of lead wire employed will depend upon the distance between the gage and the instrumentation system. For normal laboratory installations, where lengths rarely exceed 10 to 15 ft (3 to 5 m), wire sizes between 26 and 30 gage are frequently used. Stranded wire is usually preferred to solid wire since it is more flexible and suffers less breakage due to improper stripping or lead-wire movement during the test.

6.5 Gage Sensitivities and Gage Factor [22–26]

The strain sensitivity of a single, uniform length of a conductor was previously defined as

$$S_A = \frac{dR/R}{\epsilon} \approx \frac{\Delta R/R}{\epsilon} \tag{6.2}$$

where ϵ is a uniform strain along the conductor and in the direction of the axis of the conductor. This sensitivity S_A is a function of the alloy employed to fabricate the conductor and its metallurgical condition. Whenever the conductor is formed into a grid to yield the short gage length required for measuring strain, the gage exhibits a sensitivity to both axial and transverse strain.

With the older flat-grid wire gages, the transverse sensitivity was due primarily to the end loops in the grid pattern, which placed part of the conductor in the transverse direction. In the foil gages, the end loops are enlarged and thus considerably desensitized. The axial segments of the grid pattern, however, have a large width-to-thickness ratio; thus, some amount of transverse strain will be transmitted through the adhesive and carrier material to the axial segments of the grid pattern to produce a response in addition to the axial-strain response. The magnitude of the transverse strain transmitted to the grid segments depends upon the thickness and elastic modulus of the adhesive, the carrier material, the grid material, and the width-to-thickness ratio of the axial segments of the grid.

The response of a bonded strain gage to a biaxial strain field can be expressed as

$$\frac{\Delta R}{R} = S_a\epsilon_a + S_t\epsilon_t + S_s\gamma_{at} \tag{6.3}$$

where ϵ_a = normal strain along axial direction of gage
ϵ_t = normal strain along transverse direction of gage
γ_{at} = shearing strain
S_a = sensitivity of gage to axial strain
S_t = sensitivity of gage to transverse strain
S_s = sensitivity of gage to shearing strain

In general, the gage sensitivity to shearing strain is small and can be neglected. The response of the gage can then be expressed as

$$\frac{\Delta R}{R} = S_a(\epsilon_a + K_t\epsilon_t) \tag{6.4}$$

where $K_t = S_t/S_a$ is defined as the transverse sensitivity factor for the gage.

Strain-gage manufacturers provide a calibration constant known as the *gage factor* S_g for each gage. The gage factor S_g relates the resistance change to the axial strain. Thus

$$\frac{\Delta R}{R} = S_g\epsilon_a \tag{6.5}$$

The gage factor for each lot of gages produced is determined by mounting sample gages drawn from the lot on a specially designed calibration beam like that illustrated in Fig. 6.11. The beam is then deflected a specified distance to produce a known strain ϵ_a. The resistance change ΔR is then measured and the gage factor S_g is determined by using Eq. (6.5).

With this method of calibration, the strain field experienced by the gage is biaxial, with

$$\epsilon_t = -\nu_0\epsilon_a \tag{a}$$

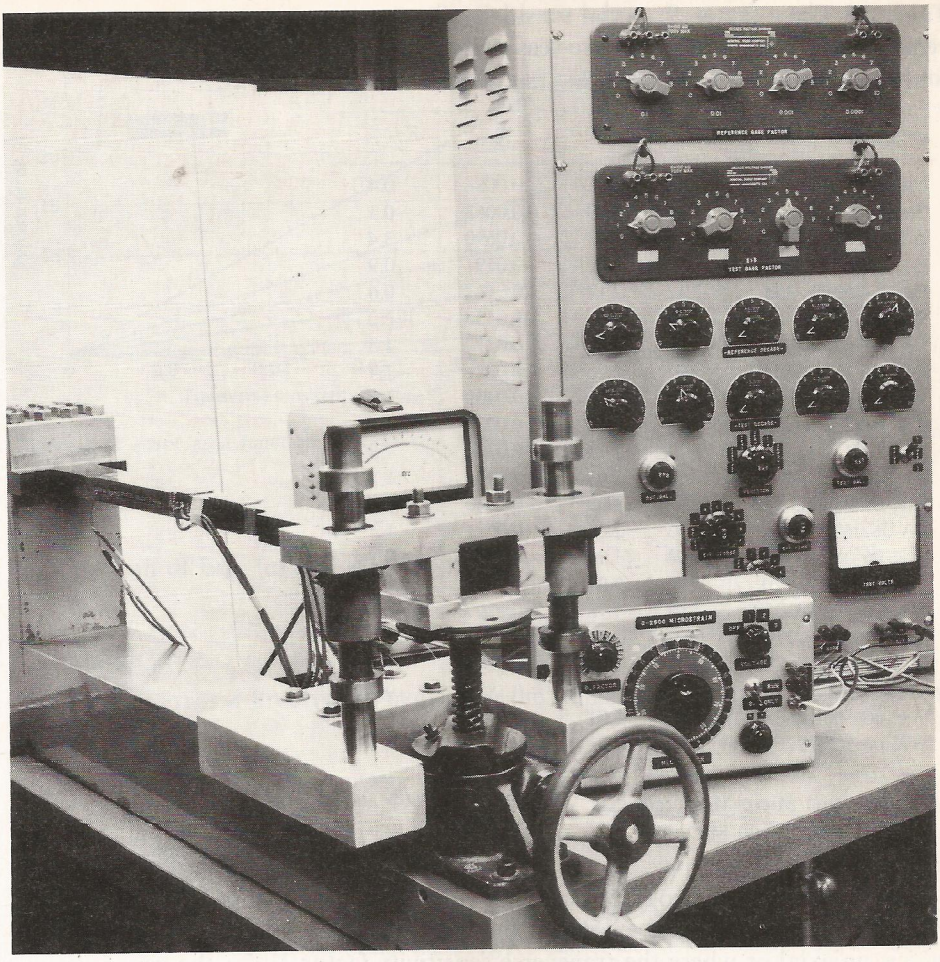

Figure 6.11 Beam and Wheatstone bridge circuits used in calibrating strain gages to determine the gage factor S_g. (*Micro-Measurements.*)

where $\nu_0 = 0.285$ is Poisson's ratio of the beam material. If Eq. (*a*) is substituted into Eq. (6.4), the resistance change in the calibration process is

$$\frac{\Delta R}{R} = S_a \epsilon_a (1 - \nu_0 K_t) \tag{6.6}$$

Since the resistance changes given by Eqs. (6.5) and (6.6) are identical, the gage factor S_g is related to both S_a and K_t by the expression

$$S_g = S_a(1 - \nu_0 K_t) \tag{6.7}$$

Typical values of S_g, S_a, and K_t for several different gage configurations are shown in Table 6.3.

Table 6.3 Gage factor S_g, axial sensitivity S_a, transverse sensitivity S_t, and transverse-sensitivity factor K_t for several different foil-type strain gages†‡

Gage type	S_g	S_a	S_t	K_t, %
EA-06-250BG-120	2.11	2.11	0.0084	0.4
WA-06-250BG-120	2.10	2.10	−0.0063	−0.3
WK-06-250BG-350	2.05	2.03	−0.0690	−3.4
EA-50-250BG-120	2.12	2.12	0.0191	0.9
EA-06-250BF-350	2.12	2.12	0.0127	0.6
WK-06-250BF-1000	2.07	2.06	−0.0453	−2.2
EA-06-125AD-120	2.10	2.11	0.0274	1.3
WK-06-125AD-350	2.07	2.06	−0.0288	−1.4
WK-15-125AD-350	2.16	2.15	−0.0409	−1.9
EA-06-125AS-500	2.14	2.14	0.0086	0.4
EA-06-015CK-120	2.13	2.14	0.0385	1.8
EA-06-030TU-120	2.02	2.03	0.0244	1.2
WK-06-030TU-350	1.98	1.98	0.0040	0.2
EA-06-062DY-120	2.03	2.04	0.0286	1.4
WK-06-062DY-350	1.96	1.96	−0.0098	−0.5
EA-06-125RA-120	2.06	2.07	0.0228	1.1
WK-06-125RA-350	1.99	1.98	−0.0297	−1.5
EA-06-500AF-120	2.09	2.09	0.0	0
WA-06-500AF-120	2.09	2.08	−0.0270	−1.3
WK-06-500AF-350	2.04	1.99	−0.1831	−9.2
WK-06-500BH-350	2.05	2.01	−0.1347	−6.7
WK-06-500BL-1000	2.06	2.03	−0.0893	−4.4

† Data from Micro-Measurements.
‡ Values depend on lot of foil.

It is important to recognize that error will occur in a strain-gage measurement when Eq. (6.5) is employed except for the two special cases where either the stress field is uniaxial or where the transverse sensitivity factor K_t for the gage is zero. The magnitude of the error can be determined by considering the response of a gage in a general biaxial field with strains ϵ_a and ϵ_t. Substituting Eq. (6.7) into Eq. (6.4) gives

$$\frac{\Delta R}{R} = \frac{S_g \epsilon_a}{1 - \nu_0 K_t}\left(1 + K_t \frac{\epsilon_t}{\epsilon_a}\right) \tag{b}$$

From Eq. (*b*), the true value of the strain ϵ_a can be expressed as

$$\epsilon_a = \frac{\Delta R/R}{S_g} \frac{1 - \nu_0 K_t}{1 + K_t(\epsilon_t/\epsilon_a)} \tag{c}$$

The apparent strain ϵ_a', which is obtained if only the gage factor is considered, can be determined from Eq. (6.5) as

$$\epsilon_a' = \frac{\Delta R/R}{S_g} \tag{d}$$

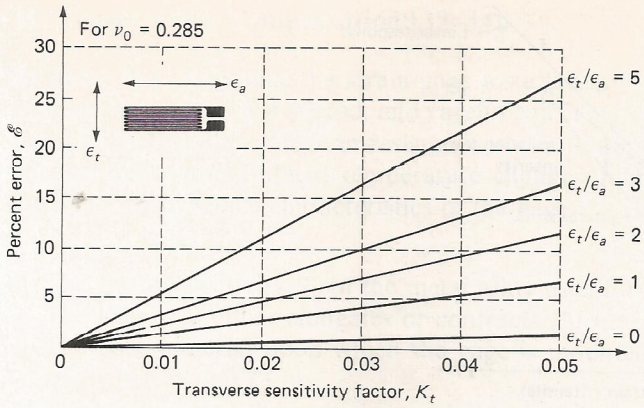

Figure 6.12 Error as a function of transverse sensitivity factor with the biaxial strain ratio as a parameter.

Comparison of Eqs. (*c*) and (*d*) shows that

$$\epsilon_a = \epsilon_a' \frac{1 - \nu_0 K_t}{1 + K_t(\epsilon_t/\epsilon_a)} \tag{6.8}$$

The percent error $\mathscr{E}$ involved in neglecting the transverse sensitivity of the gage is given by

$$\mathscr{E} = \frac{\epsilon_a' - \epsilon_a}{\epsilon_a}(100) \tag{6.9}$$

Substituting Eq. (6.8) into Eq. (6.9) yields

$$\mathscr{E} = \frac{K_t(\epsilon_t/\epsilon_a + \nu_0)}{1 - \nu_0 K_t}(100) \tag{6.10}$$

The results of Eq. (6.10), shown graphically in Fig. 6.12, indicate that the error is a function of K_t and the strain biaxiality ratio ϵ_t/ϵ_a. Since the errors can be significant when both K_t and ϵ_t/ϵ_a are large, it is important that corrections be made to account for the transverse sensitivity of the gage. Methods to correct for these errors are presented in Sec. 10.4.

6.6 PERFORMANCE CHARACTERISTICS OF FOIL STRAIN GAGES

Foil strain gages are small precision resistors mounted on a flexible carrier that can be bonded to a component part in a typical application. The gage resistance is accurate to ± 0.4 percent, and the gage factor, based on a lot calibration, is certified to ± 1.5 percent. These specifications indicate that foil-type gages provide

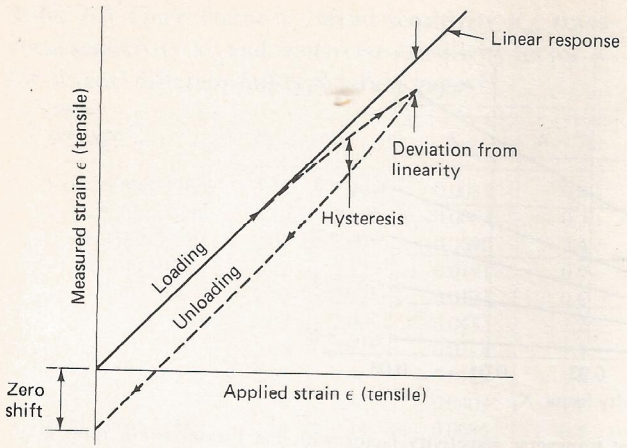

Figure 6.13 A typical strain cycle showing nonlinearity, hysteresis, and zero shift (scale exaggerated).

a means for making precise measurements of strain. The results actually obtained, however, are a function of the installation procedures, the state of strain being measured, and environmental conditions during the test. All these factors affect the performance of a strain-gage system.

A. Strain-Gage Linearity, Hysteresis, and Zero Shift [27–31]

One measure of the performance of a strain-gage system (system here implies gage, adhesive, and instrumentation) involves considerations of linearity, hysteresis, and zero shift. If gage output, in terms of measured strain, is plotted as a function of applied strain as the load on the component is cycled, results similar to those shown in Fig. 6.13 will be obtained. A slight deviation from linearity is typically observed, and the unloading curve normally falls below the loading curve to form a hysteresis loop. Also, when the applied strain is reduced to zero, the gage output indicates a small negative strain, termed *zero shift*. The magnitude of the deviation from linearity, hysteresis, and zero shift depends upon the strain level, the adequacy of the bond, the degree of cold work of the foil material, and the carrier material.

For properly installed gages, deviations from linearity should be approximately 0.1 percent of the maximum strain for polyimide carriers and 0.05 percent for epoxy carriers. First-cycle hysteresis and zero shift are more difficult to predict; however, zero shifts of 1 percent of the maximum strain are frequently observed in typical applications. If possible, strain cycling to 125 percent of the maximum test strain is recommended since the amount of hysteresis and zero shift will decrease to less than 0.2 percent of the maximum strain after 4 or 5 cycles.

B. Temperature Compensation [32–34]

In many test programs, the strain-gage installation is subjected to temperature changes during the test period, and careful consideration must be given to determining whether the change in resistance is due to applied strain or temperature change. When the ambient temperature changes, four effects occur which may alter the performance characteristics of the gage:

1. The strain sensitivity S_A of the metal alloy used for the grid changes.
2. The gage grid either elongates or contracts ($\Delta l/l = \alpha\ \Delta T$).
3. The base material upon which the gage is mounted either elongates or contracts ($\Delta l/l = \beta\ \Delta T$).
4. The resistance of the gage changes because of the influence of the temperature coefficient of resistivity of the gage material ($\Delta R/R = \gamma\ \Delta T$).

The change in the strain sensitivity S_A of Advance and Karma alloys with variations in temperature is shown in Fig. 6.14. These data indicate that $\Delta S_A/\Delta T$ equals 0.00735 and -0.00975 percent per Celsius degree for Advance and Karma alloys, respectively. As a consequence, the variations of S_A with temperature are neglected for room-temperature testing, where the temperature fluctuations rarely exceed $\pm 10°C$. In thermal-stress problems, however, larger temperature variations are possible, and the change in S_A should be taken into account by adjusting the gage factor as the temperature changes during the test period.

The effects of gage-grid elongation, base-material elongation, and increase in gage resistance with increases in temperature combine to produce a temperature-induced change in resistance of the gage $(\Delta R/R)_{\Delta T}$, which can be expressed as

$$\left(\frac{\Delta R}{R}\right)_{\Delta T} = (\beta - \alpha)S_g\ \Delta T + \gamma\ \Delta T \tag{6.11}$$

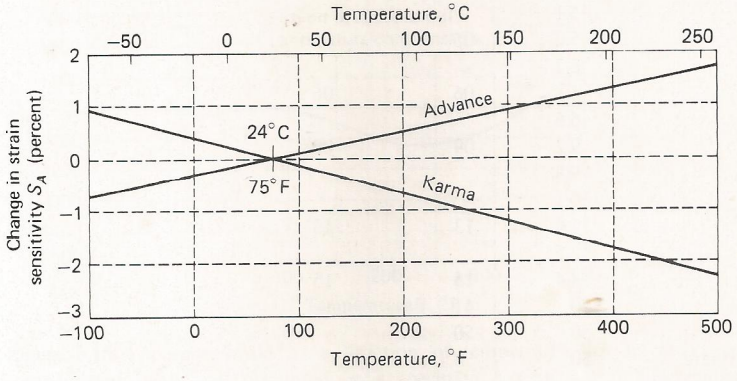

Figure 6.14 Change in alloy sensitivity S_A of Advance and Karma alloys as a function of temperature.

where α = thermal coefficient of expansion of gage material
β = thermal coefficient of expansion of base material
γ = temperature coefficient of resistivity of gage material
S_g = gage factor

If there is a differential expansion between the gage and the base material due to temperature change (that is, $\alpha \neq \beta$), the gage will be subjected to a mechanical strain $\epsilon = (\beta - \alpha)\,\Delta T$, which does not occur in the specimen. The gage reacts to this strain by indicating a change in resistance in the same manner that it indicates a change for a strain due to the load applied to the specimen. Unfortunately, it is impossible to separate the apparent strain due to the change in temperature from the strain due to the applied load. If the gage alloy and the base material have identical coefficients of expansion, this component of the thermally induced $(\Delta R/R)_{\Delta T}$ vanishes. The gage may still register a change of resistance with temperature, however, if the coefficient of resistivity γ is not zero. This component of $(\Delta R/R)_{\Delta T}$ indicates an apparent strain which does not exist in the specimen.

Two approaches can be employed to effect temperature compensation in a gage system. The first involves compensation in the gage so that the net effect of the three factors in Eq. (6.11) is canceled out. The second involves compensation for the effects of the temperature change in the electrical system required to measure the output of the gage. The second method will be discussed in Chap. 8, when electrical systems are considered in detail.

Table 6.3 Expansion coefficients available in temperature-compensated gages

Specimen material	Coefficient of expansion, $°F^{-1} \times 10^{-6}$	Self-temperature-compensating number	
		Advance	Karma
Quartz	0.3	00	00
Alumina	3.0	03	03
Zirconium	3.1		
Glass	5.0	05	05
Titanium	5.2		
Cast iron	5.8	06	06
Steel	6.6		
Stainless steel	9.2	09	09
Copper	9.8		
Bronze	10.1		
Brass	11.4	13	13
Aluminum	12.5		
Magnesium	14.4	15	15
Polystyrene	40	41	
Epoxy resin	50	50	
Polymethyl methacrylate	50		
Acrylic resin	100		

In producing temperature-compensated gages it is possible to obtain compensation by perfectly matching the coefficients of expansion of the base material and the gage alloy while holding the temperature coefficient of resistivity at zero. Compensation can also be obtained with a mismatch in the coefficients of expansion if the effect of a finite temperature coefficient of resistivity cancels out the effect of the mismatch in temperature coefficients of expansion.

The values of the factors α and γ influencing the temperature response of the strain gage mounted on a specimen with thermal characteristics specified by the value of β are quite sensitive to the composition of the strain-gage alloy, its impurities, and the degree of cold working used in its manufacture. Recently, it has become common practice for strain-gage manufacturers to determine the thermal response characteristics of sample gages from each lot of alloy material which they employ in their production. Because of variations in α and γ between each melt and each roll of foil, it is possible to select foils of Advance and Karma alloys which are suitable for use with almost any type of base material. The gages produced by using this selection technique are known as *selected-melt* or *temperature-compensated gages* and are commercially available with the self-temperature-compensating numbers listed in Table 6.3. Some widely used materials and approximate values for their temperature coefficients of expansion are also listed in the table.

Unfortunately, these gages are not perfectly compensated over a wide range in temperature because of the nonlinear character of both the expansion coefficients and the resistivity coefficients with temperature. A typical curve showing the apparent strain (temperature-induced) as a function of temperature for a temperature-compensated strain gage fabricated from Advance alloy is shown in Fig. 6.15. These results show that the errors introduced by small changes in temperature in the neighborhood of 75°F (24°C) are quite small with apparent strains

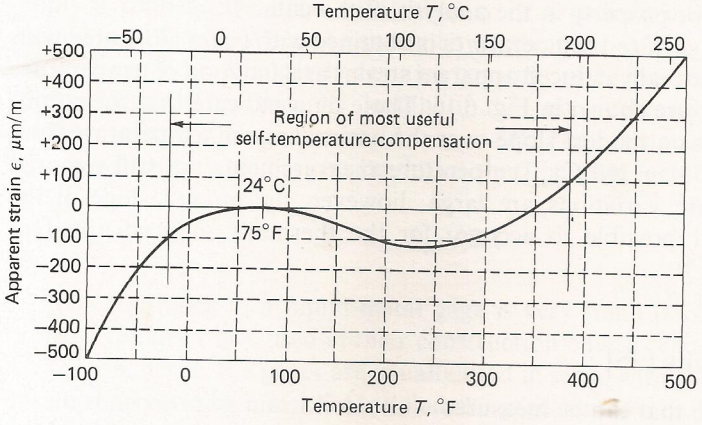

Figure 6.15 Apparent strain as a function of temperature for an Advance alloy temperature-compensated strain gage mounted on a specimen having a matching temperature coefficient of expansion.

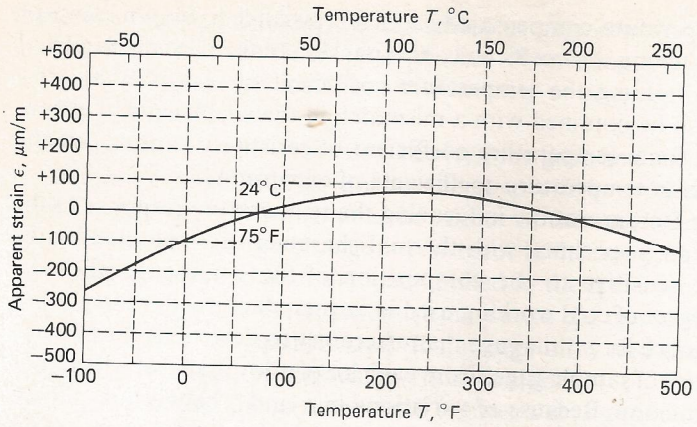

Figure 6.16 Apparent strain as a function of temperature for a Karma alloy temperature-compensated strain gage mounted on a specimen having a matching temperature coefficient of expansion.

of less than 1 μin/(in)(°F) or $\frac{1}{2}$ μm/(m)(°C). However, when the change in temperature is large, the apparent strains can become significant, and corrections to account for the thermally induced apparent strains are necessary. These corrections involve measurement of the test temperature at the gage site with a thermocouple and use of a calibration curve similar to the one shown in Fig. 6.15. A calibration curve is provided by the strain-gage manufacturer for each lot of gages produced.

The range of temperature over which an Advance alloy strain gage can be employed is approximately from −20 to 380°F (−30 to 193°C). For temperatures above and below these respective limits, the gage will function; however, very small changes in temperature will produce large apparent strains which can be difficult to account for properly in the analysis of the data.

An extended range of test temperatures is obtained with gages fabricated with Karma alloy. The thermally induced apparent strains as a function of temperature for the Karma alloy are shown in Fig. 6.16. These data indicate that the strain-temperature curve has a modest slope over the entire range of temperature from −100 to 500°F (−73 to 260°C). Temperature measurements are still required whenever temperature variations are large; however, the modest slope of the calibration makes it possible to account for the thermally induced apparent strains accurately.

C. Elongation Limits [35]

The maximum strain that can be measured with a foil strain gage depends on the gage length, the foil alloy, the carrier material, and the adhesive. The Advance and Karma alloys with polyimide carriers, used for general-purpose strain gages, can be employed to strain limits of ±5 and ±1.5 percent strain, respectively. This

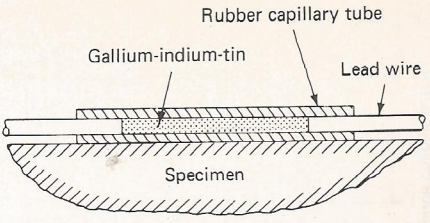

Figure 6.17 A liquid-metal electrical-resistance strain gage.

strain range is adequate for elastic analyses on metallic and ceramic components, where yield or fracture strains rarely exceed 1 percent; however, these limits can easily be exceeded in plastic analyses, where strains in the postyield range can become large. In these instances, a special postyield gage is normally employed; it is fabricated using a double annealed Advance foil grid with a high-elongation polyimide carrier. Urethane-modified epoxy adhesives are generally used to bond postyield gages to the structure. If proper care is exercised in preparing the surface of the specimen, roughening the back of the gage, formulating a high-elongation plasticized adhesive system, and attaching the lead wires without significant stress raisers, it is possible to approach strain levels of 20 percent before cracks begin to occur in the solder tabs or at the ends of the grid loops.

Special-purpose strain-gage alloys are not applicable for measurements of large strains. The Isoelastic alloy will withstand ± 2 percent strain; however, it undergoes a change of sensitivity at strains larger than 0.75 percent (see Fig. 6.2). Armour D and Nichrome V are primarily used for high-temperature measurements and are limited to maximum strain levels of approximately ± 1 percent.

For very large strains, where specimen elongations of 100 percent may be encountered, liquid-metal strain gages can be used. The liquid-metal strain gage is simply a rubber tube filled with mercury or a gallium-indium-tin alloy, as indicated in Fig. 6.17. When the specimen to which the gage is attached is strained, the volume of the tube cavity remains constant since Poisson's ratio of rubber is approximately 0.5. Thus the length of the tube increases ($\Delta l = \epsilon l$) while the diameter of the tube decreases ($\Delta d = -\nu \epsilon d$). The resistance of such a gage increases with strain, and it can be shown that the gage factor is given by

$$S_g = 2 + \epsilon \tag{6.12}$$

The resistance of a liquid-metal gage is very small (less than 1 Ω) since the rubber capillary tubes used in their construction have a relatively large diameter. As a consequence, the gages are usually used in series with a large fixed resistor to form a total resistance of 120 Ω so that the gage can be monitored with a conventional Wheatstone bridge. The response of a liquid-metal gage, as shown in Fig. 6.18, is slightly nonlinear with increasing strain due to the increase in gage factor with strain.

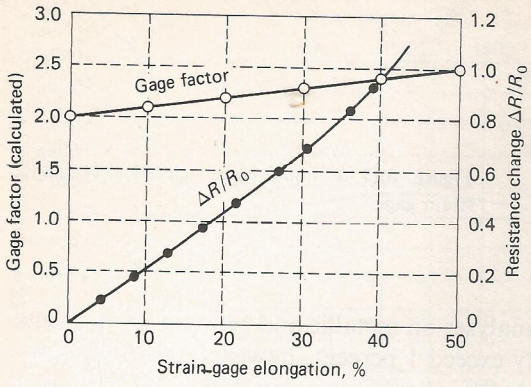

Figure 6.18 Resistance change and gage factor as a function of strain for a liquid-metal strain gage (from data by Harding).

D. Dynamic Response of Strain Gages [36–39]

In dynamic applications of strain gages, the question of their frequency response often arises. This question can be resolved into two parts, namely, the response of the gage in its thickness direction, i.e., how long it takes for an element of the gage to respond to the strain in the specimen beneath it, and the response of the gage due to its length. It is possible to estimate the time required to transmit the strain from the specimen through the adhesive and carrier to the strain-sensing element by considering a gage mounted on a specimen as shown in Fig. 6.19. A strain wave is propagating through the specimen with velocity c_1. This specimen strain wave induces a shear-strain wave in the adhesive and carrier which propagates with a velocity c_2. The transit time, which is given by $t = h/c_2$, equals 5×10^{-8} s for typical carrier and adhesive combinations, where $c_2 = 40{,}000$ in/s (1000 m/s) and $h = 0.002$ in (0.05 mm). The time required for the conductor to respond may exceed this transit time by a factor of 3 to 5; therefore, the response time should be approximately 2×10^{-7} s. Experiments conducted by Oi and an analysis by Bickle indicate that transit times are approximately 0.1 μs.

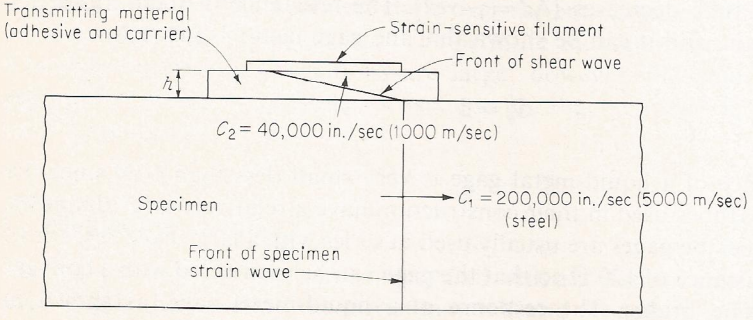

Figure 6.19 Dynamic strain transmission between the specimen and the gage.

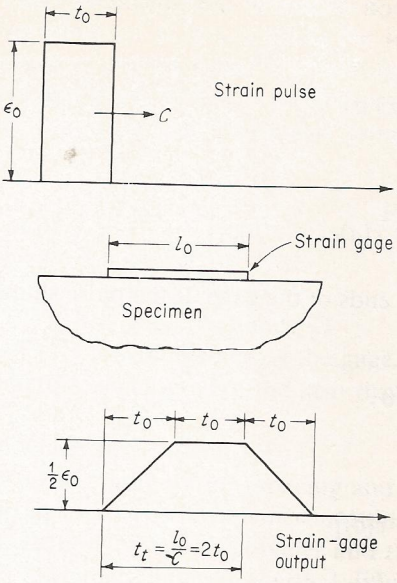

Figure 6.20 Dynamic response of a gage due to a step-pulse input.

The rise time for a strain gage responding to a step pulse is given by

$$t_r = \frac{l_0}{c_1} + 0.1 \times 10^{-6} \tag{6.13}$$

where l_0 is the length of the gage and the 0.1-μs term is added to account for the transmission time through the carrier and adhesive. A typical rise time for a 0.125-in (3.17-mm) gage mounted on a steel bar ($c_1 = 200{,}000$ in/s or 5000 m/s) is $0.6 + 0.1 = 0.7$ μs. Such short rise times are often neglected when long strain pulses are encountered and the rate of change of strain with time is small. When short, steep-fronted strain pulses are encountered, however, the response time of the gage should be considered since the measured strain pulse can be distorted, as shown in Fig. 6.20. In this instance, the gage is mounted on a specimen which is propagating a strain pulse having an amplitude ϵ_0, a time duration t_0, and a velocity c. The front of the pulse will reach and just pass over a gage of length l_0 in a transit time $t_t = l_0/c$. In Fig. 6.20 the transit time t_t equals $2t_0$. If the gage records average strain over its length, its output will rise linearly to a value of $\epsilon_0/2$ over a time period of t_0. The output will then remain constant at $\epsilon_0/2$ for a period of time equal to t_0 and then decrease linearly to zero over a final time period of t_0. The effect of the gage length in this example was to decrease the amplitude of the output by a factor of 2 and to increase the total time duration of the pulse by a factor of 3. The distortion of the pulse as indicated by the gage will depend upon the ratio t_t/t_0; and as the value of this ratio goes to zero, the distortion vanishes.

It is also possible to correct for this distortion. Note that the indicated strain $\bar{\epsilon}$ at time t is given by

$$\bar{\epsilon}(t) = \frac{1}{l_0} \int_{c_1 t - l_0}^{c_1 t} \epsilon(x)\, dx \tag{6.14}$$

Differentiating gives

$$\frac{d\bar{\epsilon}}{dt} = \frac{1}{l_0} \left\{ \int_{c_1 t - l_0}^{c_1 t} \frac{\partial}{\partial t}[\epsilon(x)]\, dx + \epsilon(a)c_1 - \epsilon(b)c_1 \right\} \tag{6.15}$$

where $\epsilon(a)$ and $\epsilon(b)$ are the strains at the two ends of the gage. If the pulse shape remains constant during propagation,

$$\frac{\partial}{\partial t}[\epsilon(x)] = 0$$

and Eq. (6.15) reduces to

$$\frac{d\bar{\epsilon}}{dt} = \frac{c_1}{l_0}[\epsilon(a) - \epsilon(b)] \tag{6.16}$$

Since

$$\epsilon(b, t) = \epsilon\left(a, t - \frac{l_0}{c_1}\right)$$

then

$$\epsilon(a, t) = \frac{l_0}{c_1}\frac{d\epsilon}{dt} + \epsilon\left(a, t - \frac{l_0}{c_1}\right) \tag{6.17}$$

An analog circuit can be constructed using operational amplifiers to automatically correct the signal output from the gage as given by Eq. (6.17). The block diagram for such an analog circuit is given in Fig. 6.21.

E. Heat Dissipation [40–43]

It is well recognized that temperature variations can significantly influence the output of strain gages, particularly those which are not temperature-compensated. The temperature of the gage is of course influenced by ambient-temperature variations and by the power dissipated in the gage when it is connected into a Wheatstone bridge or a potentiometer circuit. The power P is dissipated in the form of

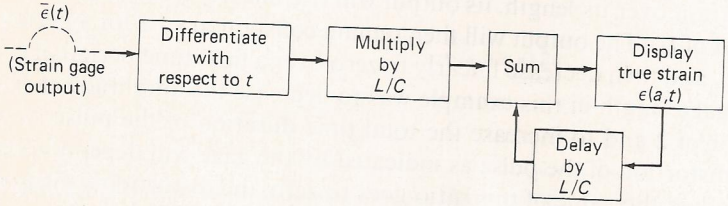

Figure 6.21 Analog circuit which eliminates pulse distortion due to strain-gage length. (*After Bickle.*)

heat; therefore, the temperature of the gage must increase above the ambient temperature to accomplish the heat transfer. The exact temperature increase required is very difficult to specify since many factors influence the heat balance for the gage. The heat to be dissipated depends upon the voltage applied to the gage and the gage resistance. Thus

$$P = \frac{V^2}{R} = I^2 R \tag{6.18}$$

where P = power, W
I = gage current, A
R = gage resistance, Ω
V = voltage across the gage, V

Factors which govern the heat dissipation include

1. Gage size, w_0 and l_0
2. Grid configuration, spacing and size of conducting elements
3. Carrier, type of polymer and thickness
4. Adhesive, type of polymer and thickness
5. Specimen material, thermal diffusivity
6. Specimen volume in the local area of the gage
7. Type and thickness of overcoat used to waterproof the gage
8. Velocity of the air flowing over the gage installation

A parameter often used to characterize the heat-dissipation characteristics of a strain-gage installation is the power density P_D, which is defined as

$$P_D = \frac{P}{A} \tag{6.19}$$

where P is the power that must be dissipated by the gage and A is the area of the grid of the gage. Power densities that can be tolerated by a gage are strongly related to the specimen which serves as the heat sink. Recommended values of P_D for different materials and conditions are listed in Table 6.4.

Table 6.4 Allowable power densities

Power density P_D		
W/in^2	W/mm^2	Specimen conditions
5–10	0.008–0.016	Heavy aluminum or copper sections
2–5	0.003–0.008	Heavy steel sections
1–2	0.0015–0.003	Thin steel sections
0.2–0.5	0.0003–0.0008	Fiber glass, glass, ceramics
0.02–0.05	0.00003–0.00008	Unfilled plastics

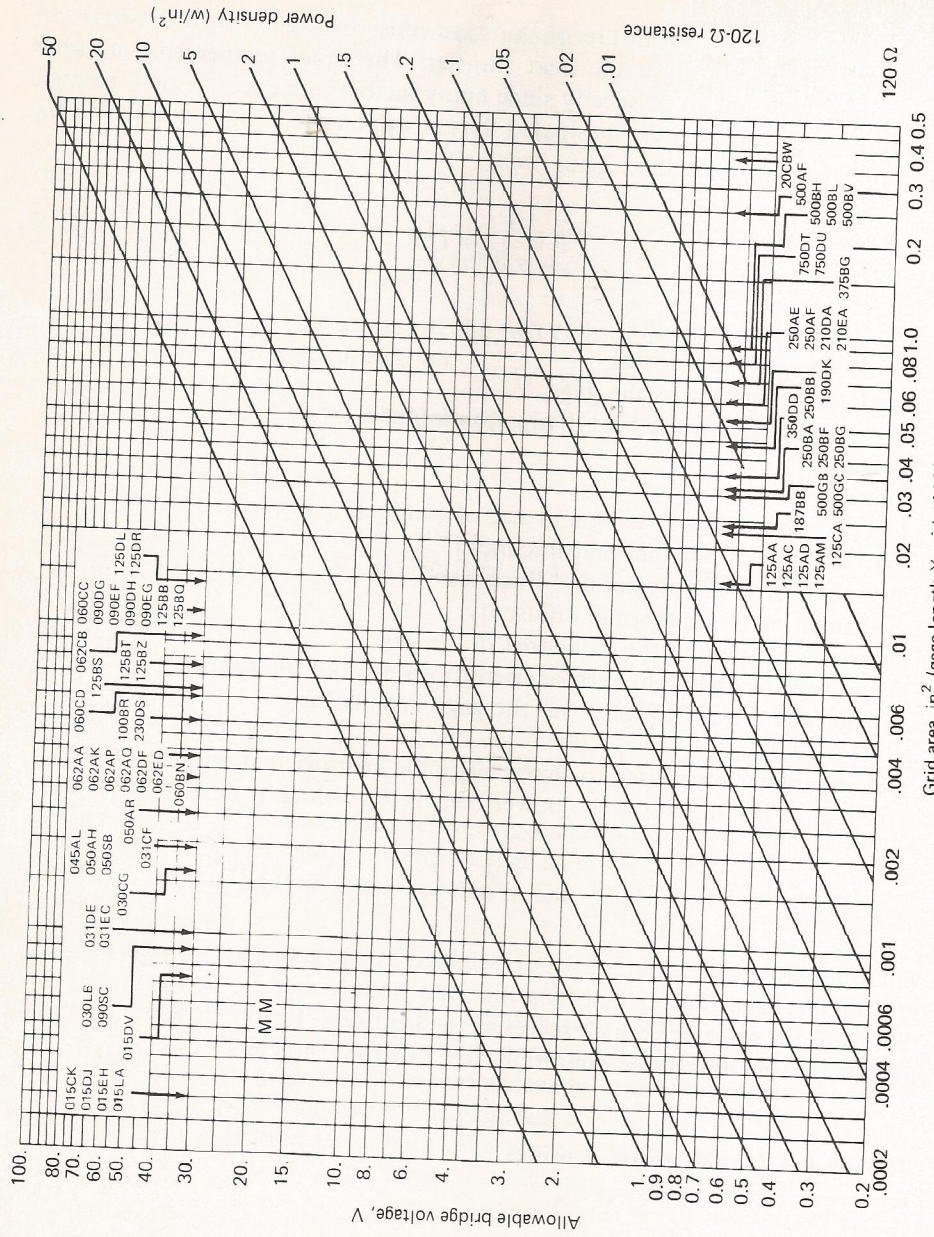

Figure 6.22 Allowable bridge voltage as a function of grid area with power density as a parameter for 120-Ω electrical-resistance strain gages. (*Micro-Measurements.*)

When a Wheatstone bridge with four equal arms is employed, the bridge excitation voltage V_B is related to the power density on the strain gage by

$$V_B^2 = 4AP_D R \tag{6.20}$$

Allowable bridge voltages for specified grid areas and power densities are shown for 120-Ω gages in Fig. 6.22. Typical grid configurations are identified along the abscissa in the figure to illustrate the effect of gage size on allowable bridge excitation. It should be noted that small gages mounted on a poor heat sink ($P_D < 1$ W/in^2 or 0.0015 W/mm^2) result in lower allowable bridge voltages than those employed in most commercial strain indicators (3 to 5 V). In these instances it is necessary to use a higher-resistance gage (350 Ω in place of 120 Ω), a gage with a larger grid area, or a fixed resistor in series with the gage to reduce the voltage on the gage in both the active and compensating arms of the bridge.

F. Stability [44–47]

In certain strain-gage applications it is necessary to record strains over a period of months or years without having the opportunity to unload the specimen and recheck the zero reading. The duration of the readout period is important and makes this application of strain gages one of the most difficult. All the factors which can influence the behavior of the gage have an opportunity to do so; moreover, there is enough time for the individual contribution to the error from each of the factors to become quite significant. For this reason it is imperative that every precaution be taken in employing the resistance-type gage if meaningful data are to be obtained.

Drift in the zero reading from an electrical-resistance strain-gage installation is due to the effects of moisture or humidity variations on the carrier and the adhesive, the effects of long-term stress relaxation of the adhesive, the carrier, and the strain-gage alloy, and the instabilities in the resistors in the inactive arms of the Wheatstone bridge.

Results of an interesting series of stability tests by Freynik are presented in Fig. 6.23. In evaluating a typical general-purpose strain gage with a grid fabricated from Advance alloy and a polyimide carrier, zero shifts of 270 μin/in (μm/m) were observed after 30 days. Since this installation was carefully waterproofed, the large drifts were attributed to stress relaxation in the polyimide carrier over the period of observation.

Results from a second strain-gage installation with a grid fabricated from Advance alloy and a carrier from glass-fiber-reinforced phenolic were more satisfactory with zero drift of approximately 100 μin/in (μm/m) after 50 days. The presence of the glass fibers essentially eliminated drift due to stress relaxation in the carrier material; the drift measured was attributed to instabilities in the Advance alloy grid at the test temperature of 167°F (75°C). The final and most satisfactory results were obtained with a Karma grid and an encapsulating glass-reinforced epoxy-phenolic carrier. In this case, the zero shift averaged only 30 μin/in (μm/m) after an observation period of 900 days. In similar tests with this

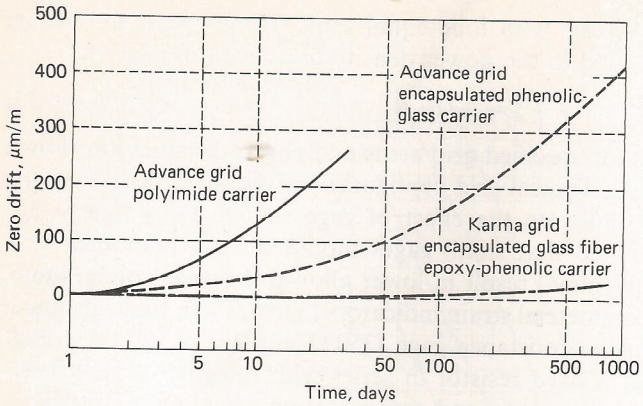

Figure 6.23 Zero drift as a function of time for several gage types at 167°F (75°C) (from data by Freynik).

gage installation at room temperature, the zero drift was only -25 μin/in (μm/m). These results show that electrical-resistance strain gages can be used for long-term measurements provided Karma grids with glass-fiber-reinforced epoxy-phenolic carriers are employed with a well-cured epoxy adhesive system. The gage installation should be waterproofed to minimize the effects of humidity. It is also important to specify hermatically sealed bridge-completion resistors to ensure stability of the bridge over the long observation periods.

6.7 ENVIRONMENTAL EFFECTS

The performance of resistance strain gages is markedly affected by the environment. Moisture, temperature extremes, hydrostatic pressure, nuclear radiation, and cyclic loading produce changes in gage behavior which must be accounted for in the installation of the gage and in the analysis of the data to obtain meaningful results. Each of these parameters is discussed in the following subsections.

A. Effects of Moisture and Humidity [48–50]

A strain-gage installation can be detrimentally affected by direct contact with water or by the water vapor normally present in the air. The water is absorbed by both the adhesive and the carrier, and the gage performance is affected in several ways. First, the moisture decreases the gage-to-ground resistance. If this value of resistance is reduced sufficiently, the effect is the same as that of placing a shunt resistor across the active gage. The water also degrades the strength and rigidity of the bond and reduces the effectiveness of the adhesive in transmitting the strain from the specimen to the gage. If this loss in adhesive strength or rigidity is

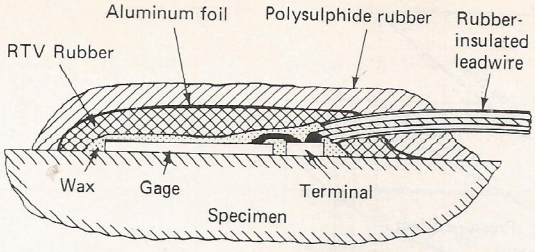

Figure 6.24 Waterproofing a gage for severe seawater exposure.

sufficient, the gage will not develop its stated calibration factors and measuring errors are introduced.

Plastics also expand when they absorb water and contract when they release it; thus, any change in the moisture concentration in the adhesive will produce strains in the adhesive, which will in turn be transmitted to the strain gage. These moisture-induced adhesive strains will produce a strain-gage response that cannot be separated from the response due to the applied mechanical strain. Finally, the presence of water in the adhesive will cause electrolysis when current passes through the gage. During the electrolysis process, the gage filament will erode and a significant increase in resistance will occur. Again, the strain gage will indicate a tensile strain due to this electrolysis which cannot be differentiated from the applied mechanical strain.

Many methods for waterproofing strain gages have been developed; however, the extent of the measures taken to protect the gage from moisture depends to a large degree on the application and the extent of the gage exposure to water. For normal laboratory work, where the readout time is relatively short, a thin layer of microcrystalline wax or an air-drying polyurethane coating is usually sufficient to protect the gage installation from moisture in the air. For much more severe applications, e.g., prolonged exposure to seawater, it is necessary to build up a seal out of soft wax, synthetic rubber, metal foil, and a final coat of rubber. A cross section of a well-protected gage installation is shown in Fig. 6.24. Care should be exercised in forming the seal at the lead-wire terminal since the seal usually fails at this location. Also, the insulation for the lead wires should be rubber, and splices in the cable should be avoided.

B. Effects of Hydrostatic Pressure [51–55]

In the stress analysis of pressure vessels and piping systems, strain gages are frequently employed on interior surfaces where they are exposed to a gas or fluid pressure which acts directly on the sensing element of the gage. Under such conditions, pressure-induced resistance changes occur which must be accounted for in the analysis of the strain-gage data.

Milligan and Brace independently studied this effect of pressure by mounting a gage on a small specimen, placing the specimen in a special high-pressure vessel,

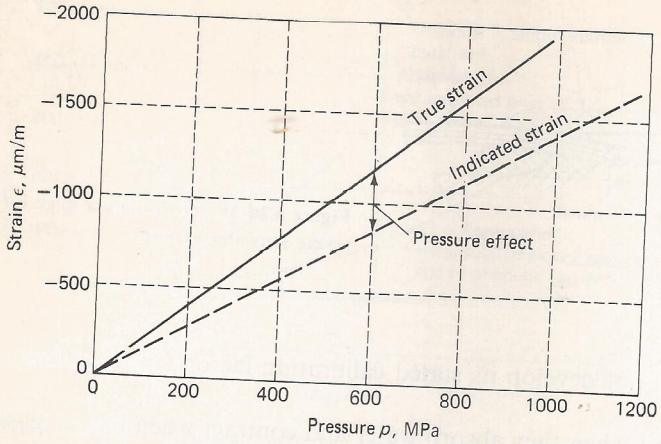

Figure 6.25 True and indicated strain as a function of pressure for an Advance foil gage with epoxy backing on a hydrostatically loaded specimen of Armco iron (from data by Brace).

and monitoring the strain as the pressure was increased to 140,000 lb/in^2 (965 MPa). In this type of experiment, the hydrostatic pressure p produces a strain in the specimen which is given by Eq. (2.16) as

$$\epsilon = \frac{-p}{E} - \frac{\nu}{E}[(-p) + (-p)] = -\frac{1-2\nu}{E}p = K_T p \tag{6.21}$$

where $K_T = -(1-2\nu)/E$ is often referred to as the *compressibility constant* for a material. The strain gages were monitored during the pressure cycle, and it was observed that the indicated strains were less than the true strains predicted by Eq. (6.21). Some typical results are shown in Fig. 6.25. The difference between the true strains and the indicated strains was attributed to the pressure effect.

The pressure effect can be characterized by defining the slope of the indicated pressure-strain curve as an apparent compressibility constant for the material. Thus

$$K_I = -\frac{\Delta\epsilon}{\Delta p} \tag{6.22}$$

The difference due to pressure D_p can then be computed as

$$D_p = \frac{K_T - K_I}{K_T} \tag{6.23}$$

Experimental results by Milligan, shown in Fig. 6.26, indicate that D_p depends upon the compressibility constant for the specimen material, the curvature of the specimen where the gage is mounted, and the type of strain-sensing alloy used in fabricating the gage. In spite of relatively large values for D_p, however, it was observed that the pressure-strain response of the gage remained linear.

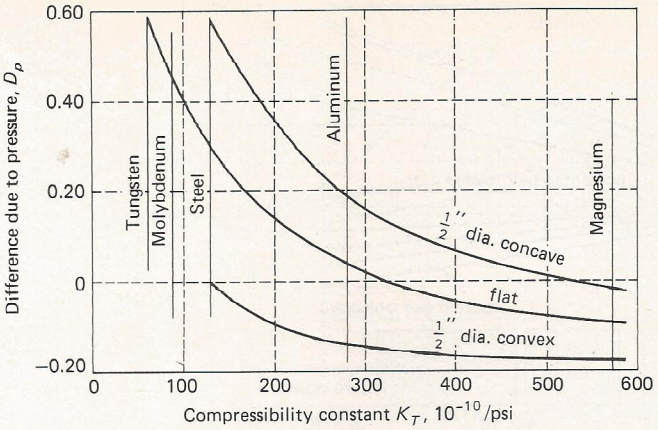

Figure 6.26 Difference due to pressure D_p as a function of compressibility constant K_T for Advance foil gages on specimens with different curvatures (from data by Milligan).

Thus, true strain can be expressed in terms of indicated strain and a correction term

$$\epsilon_t = \epsilon_i - \epsilon_{cp} \tag{6.24}$$

The magnitude of the correction term ϵ_{cp} can be expressed in terms of the experimentally determined values of D_p as

$$\epsilon_{cp} = D_p K_T p \tag{6.25}$$

For a flat steel specimen, $K_T = 133 \times 10^{-10}$ in^2/lb (1.93×10^{-12} m^2/N) and $D_p = 0.3$; hence, the correction term for the strain is approximately 4 μin/in (μm/m) for a pressure of 1000 lb/in^2 (7 MPa). Since this is a very small correction, it is possible to neglect pressure effects for pressures less than approximately 3000 lb/in^2 (20 MPa).

For hydrostatic pressure applications, foil strain gages with the thinnest possible carriers should be employed. The gage should be mounted on a smooth surface with a thinned adhesive to obtain the thinnest possible bond line. Bubbles in the adhesive layer cannot be tolerated since the pressure normal to the surface of the gage will force the sensing element into any void beneath the gage and erroneous resistance changes will result.

C. Effects of Nuclear Radiation [56–58]

Several difficult problems are encountered when electrical-resistance strain gages are employed in nuclear-radiation fields. The most serious difficulty involves the change in electrical resistivity of the strain gage and lead wires as a result of the fast-neutron dose. This effect is significant; changes of 2 to 3 percent in $\Delta R/R$ have been observed with a neutron dose of 10^{18} *nvt*. These changes in resistivity produce

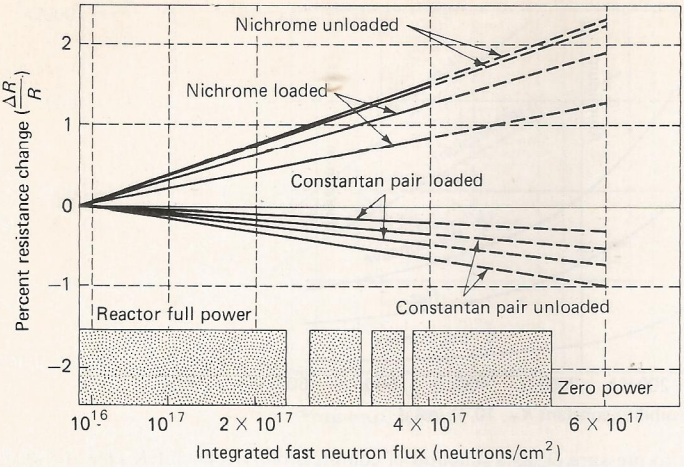

Figure 6.27 Percent resistance change as a function of exposure to neutron flux (from data by Tallman).

zero drift with time which can be as large as an apparent strain of 10,000 to 15,000 μin/in (μm/m). The exact rate of change of resistivity is a function of the strain-gage and lead-wire materials, the state of strain in the gage, and the temperature. Typical changes in resistance with integrated fast-neutron flux are shown in Fig. 6.27. Since the changes in resistivity are a function of the magnitude and sign of the strain, the use of dummy gages to cancel the effects of radiation exposure is not effective. Since the change in electrical resistivity appears to be a linear function of the logarithm of the dose, the most satisfactory solution to neutron-induced zero drift is to employ preexposed strain-gage installations and to reduce test times to a minimum. Unloading and reestablishing the zero resistance of the gage is essential.

The neutrons also produce a change in the sensitivity of the strain-gage alloys. Typical variations in S_A for Advance alloy, shown in Fig. 6.28, range from 15 to -10 percent as the integrated neutron exposure increases from 10^{16} to $6 \times 10^{17} nvt$.

The fast neutrons also produce mechanical effects which are detrimental to strain-gage installations. With exposure to the fast neutrons, the strain-gage alloy exhibits an increase in its yield strength and modulus of elasticity and a decrease in elongation capability. Radiation-induced cross-linking in polymers also destroys the original organic structure of the bond. For this reason, ceramic adhesives are normally employed in any long-term tests where exposure will accumulate.

In nuclear-radiation fields with high gamma flux, considerable energy is transferred to the gage and specimen; therefore, temperature changes can be significant. For precise measurements, the temperature change must be predicted or determined so that the strain-gage results can be corrected for the effects of temperature.

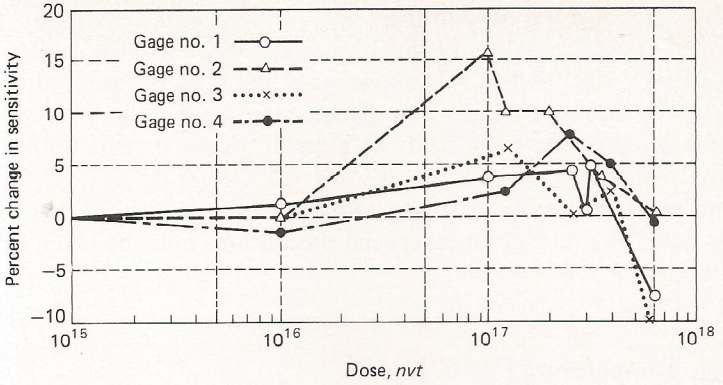

Figure 6.28 Percent change in sensitivity of an Advance alloy strain gage with exposure to fast neutrons (from data by Tallman).

Electromagnetic effects are important when the strain-gage circuit is subjected to transient flux fields for short periods of time. If gamma particles are present, potential differences of several thousand volts can be generated. The specimen must be adequately grounded to prevent the development of these high voltages.

Transient radiation pulses also produce Compton replacement currents, which are injected into the strain-gage circuit by the lead wires and the strain gages. The Compton effect results from an unbalance between the number of electrons being captured and the number being emitted by the cable conductor. These currents, when injected into the Wheatstone bridge circuit, produce spurious output signals which can be misinterpreted as strain pulses.

There are two precautions which can be taken to minimize the effects of Compton replacement currents. (1) Coaxial cables can be used for the lead wires. The shields on these conductors are effective in limiting the injected currents on the center conductor. (2) The compensating Wheatstone bridge circuit, shown in Fig. 6.29, can be used to reduce the output signal generated by the injected currents I_1, I_2, and I_3. If the active strain gage is placed in arm R_1 and the dummy

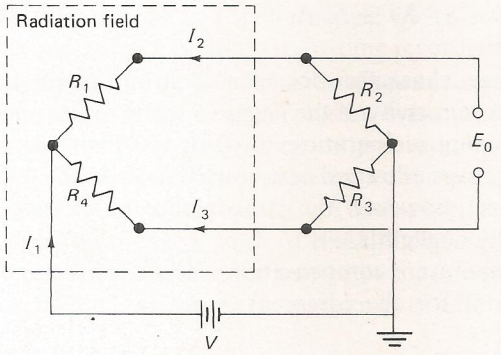

Figure 6.29 Compensating Wheatstone bridge to reduce the effects of Compton replacement currents.

gage in arm R_4, both gages are exposed to the same radiation transient and the effects of the injection currents I_1, I_2, and I_3 are minimized. The current I_1 finds a balanced path through $R_1 + R_2$ and $R_4 + R_3$ to ground and does not generate a differential voltage E_0. Currents I_2 and I_3 are equal since gages R_1 and R_4 are identical and are subjected to the same field. As a result, these currents do not produce a differential voltage E_0.

It is possible to measure strains in strong radiation fields which are either transient or steady-state. In either instance, special precautions must be taken or serious errors will occur.

D. Effects of High Temperature [59–67]

Resistance-type strain gages can be employed at elevated temperatures for both static and dynamic stress analyses; however, the measurements require many special precautions which depend primarily on the temperature and the time of observation. At elevated temperatures, the resistance R of a strain gage must be considered to be a function of temperature T and time t in addition to strain ϵ. Thus

$$R = f(\epsilon, T, t) \tag{6.26}$$

The resistance change $\Delta R/R$ is then given by

$$\frac{\Delta R}{R} = \frac{1}{R}\frac{\partial f}{\partial \epsilon}\Delta\epsilon + \frac{1}{R}\frac{\partial f}{\partial T}\Delta T + \frac{1}{R}\frac{\partial f}{\partial t}\Delta t \tag{6.27}$$

where $\dfrac{1}{R}\dfrac{\partial f}{\partial \epsilon} = S_g$ = gage sensitivity to strain (gage factor)

$\dfrac{1}{R}\dfrac{\partial f}{\partial T} = S_T$ = gage sensitivity to temperature

$\dfrac{1}{R}\dfrac{\partial f}{\partial t} = S_t$ = gage sensitivity to time

Equation (6.27) can then be expressed in terms of the three sensitivity factors as

$$\frac{\Delta R}{R} = S_g\,\Delta\epsilon + S_T\,\Delta T + S_t\,\Delta t \tag{6.28}$$

In the discussion of performance characteristics of foil strain gages in Secs. 6.5B and 6.5F, it was shown that sensitivity of the gages to temperature and time was minimized at normal operating temperatures of 0 to 150°F (−18 to 65°C) by proper selection of the strain-gage alloy and carrier materials. As the test temperature increases above this level, however, the performance of the gage changes, and S_T and S_t are not usually negligible.

As the temperature increases, temperature compensation is less effective, and corrections must be made to account for the apparent strain, as shown in

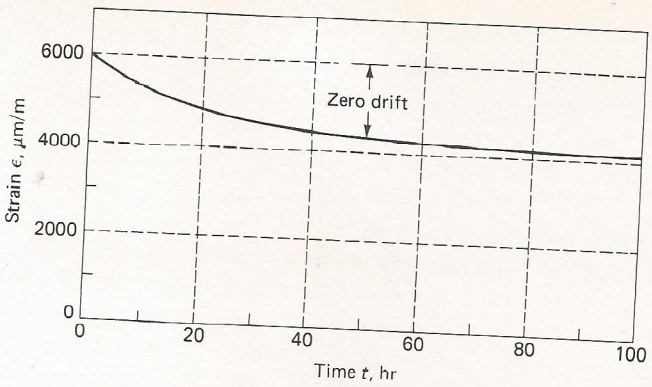

Figure 6.30 Typical zero drift as a function of time for a Karma alloy strain gage with a glass-fiber–epoxy–phenolic carrier at 560°F (293°C) (from data by Hayes).

Figs. 6.15 and 6.16. Comparisons of these results indicate that the Karma strain-gage alloy is more suitable for the higher-temperature applications than Advance. The Karma gages can be employed to temperatures up to about 500°F (260°C) without encountering excessively large temperature-induced apparent strains.

The stability of a strain-gage installation is also affected by temperature; and strain-gage drift becomes a more serious problem as the temperature and the time of observation are increased. Stability is affected by stress relaxation in the adhesive bond and in the carrier material and by metallurgical changes (phase transformations and annealing) in the strain-gage alloy. The upper temperature limit on commercially available Karma gages is controlled by the carrier material. Glass-reinforced epoxy-phenolic carriers are rated at 550°F (288°C); however, Karma gages with this type of carrier drift with time as shown in Fig. 6.30. If the time of loading and observation is long, corrections must be made for the zero drift. Drift rates will depend upon both the strain level and the temperature. For high-temperature strain analyses, it is recommended that a series of strain-time calibration curves, similar to the one shown in Fig. 6.30, be developed to cover the range of strains and temperatures to be encountered. Zero-drift corrections can then be taken from the appropriate curve.

The problem of gage stability and apparent strain due to temperature changes is greatly reduced if the period of observation is short. For dynamic analyses, where relatively short strain-time records are used (times usually less than 1 s), the temperature does not have sufficient time to change and temperature effects are therefore small. For this reason, dynamic strain-gage analyses can be made at very high temperatures with good precision and with relative ease.

Resistance-strain-gage measurements at temperatures higher than 550°F (288°C) require special gages and special techniques for mounting and monitoring the strain-gage signal. At these higher temperatures, polymeric materials can no longer be used for the carrier or the adhesive. The gages must be mounted to the specimen with the ceramic cements described in Sec. 6.4D. The carrier is either

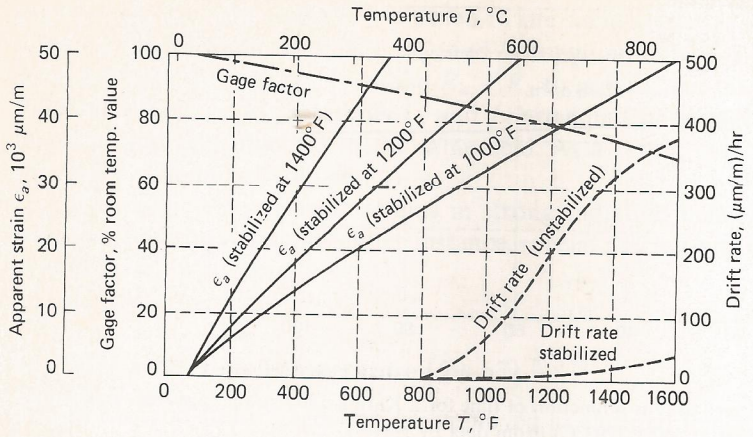

Figure 6.31 Performance characteristics of a platinum-tungsten alloy strain gage as a function of temperature (from data by Wnuk).

removed entirely or replaced with a thin stainless-steel shim. Strain gages for the very high temperature applications are fabricated using materials such as Armour D (70 Fe, 20 Cr, and 10 Al) or alloy 479 (92 Pt and 8 W).

Most commercially available strain gages rated for high-temperature use are fabricated from the platinum-tungsten alloy because of its inherent oxidation resistance and metallurgical stability. Performance characteristics of this alloy are shown as a function of temperature in Fig. 6.31. These results indicate that the gage factor drops about 30 percent as the temperature increases from 70 to 1600°F

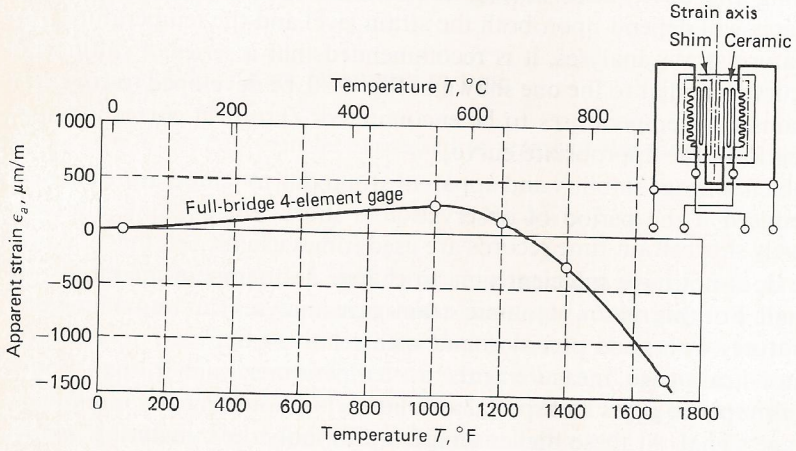

Figure 6.32 Apparent strain as a function of temperature for a four-element full-bridge gage (from data by Wnuk).

(21 to 871°C). Also, the temperature coefficient of resistance of this alloy is very high; therefore, large apparent strains [40 to 80 μin/(in)(°F) or 70 to 140 μm/(m)(°C)] are indicated by the gage when the temperature changes. The material is stable, and zero drift is negligible to temperatures of 800°F (427°C). At temperatures above 800°F (427°C), drift will occur, the rate of drift increasing with temperature.

The effects of drift rate can be minimized by stabilizing the alloy. The stabilization process consists of annealing the alloy at the test temperature for 12 to 16 h. The stabilized drift is relatively low, with rates of 20 μin/(in)(h) or μm/(m)(h) reported at 1400°F (760°C). The effect of apparent strain is much more difficult to treat and usually requires the use of dual-element or four-element gages, which compensate for the effects of temperature by signal subtraction in the Wheatstone bridge.

An example of apparent strain as a function of temperature for a four-element (complete-bridge) gage is shown in Fig. 6.32. Temperature compensation has been achieved for temperatures less than approximately 1400°F (760°C). The gage can be used at higher temperatures by correcting for apparent strain if the ceramic adhesive continues to perform adequately.

E. Effects of Cryogenic Temperatures [68–70]

Strain can be measured with electrical-resistance strain gages to liquid-nitrogen temperatures (−320°F or −196°C) and below. Two factors must be carefully accounted for in using strain gages at this temperature extreme. The first effect is the change in gage factor with temperature, illustrated in Fig. 6.33. These results

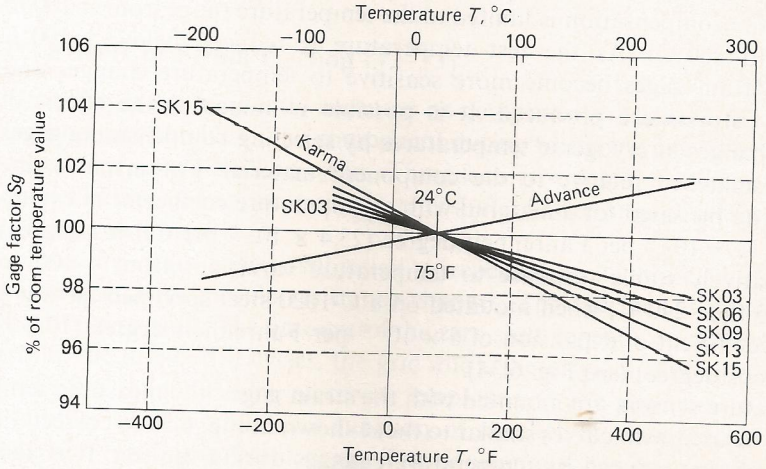

Figure 6.33 Changes in gage factor with temperature (from data by Telinde).

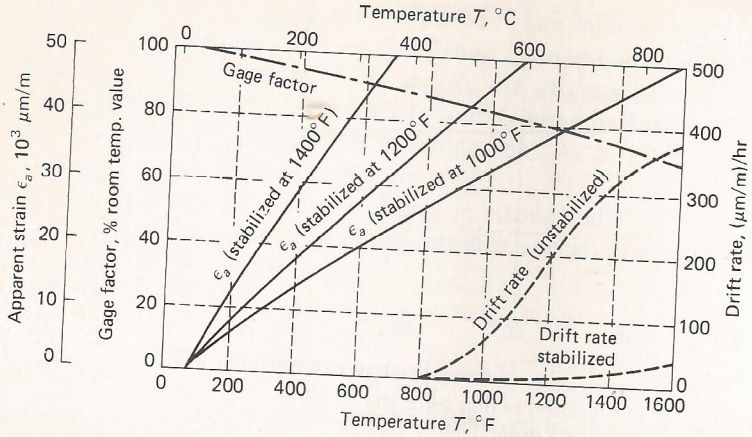

Figure 6.31 Performance characteristics of a platinum-tungsten alloy strain gage as a function of temperature (from data by Wnuk).

removed entirely or replaced with a thin stainless-steel shim. Strain gages for the very high temperature applications are fabricated using materials such as Armour D (70 Fe, 20 Cr, and 10 Al) or alloy 479 (92 Pt and 8 W).

Most commercially available strain gages rated for high-temperature use are fabricated from the platinum-tungsten alloy because of its inherent oxidation resistance and metallurgical stability. Performance characteristics of this alloy are shown as a function of temperature in Fig. 6.31. These results indicate that the gage factor drops about 30 percent as the temperature increases from 70 to 1600°F

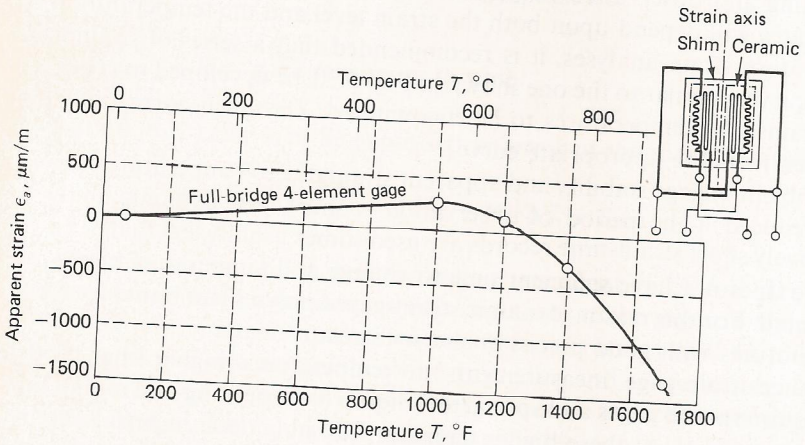

Figure 6.32 Apparent strain as a function of temperature for a four-element full-bridge gage (from data by Wnuk).

(21 to 871°C). Also, the temperature coefficient of resistance of this alloy is very high; therefore, large apparent strains [40 to 80 μin/(in)(°F) or 70 to 140 μm/(m)(°C)] are indicated by the gage when the temperature changes. The material is stable, and zero drift is negligible to temperatures of 800°F (427°C). At temperatures above 800°F (427°C), drift will occur, the rate of drift increasing with temperature.

The effects of drift rate can be minimized by stabilizing the alloy. The stabilization process consists of annealing the alloy at the test temperature for 12 to 16 h. The stabilized drift is relatively low, with rates of 20 μin/(in)(h) or μm/(m)(h) reported at 1400°F (760°C). The effect of apparent strain is much more difficult to treat and usually requires the use of dual-element or four-element gages, which compensate for the effects of temperature by signal subtraction in the Wheatstone bridge.

An example of apparent strain as a function of temperature for a four-element (complete-bridge) gage is shown in Fig. 6.32. Temperature compensation has been achieved for temperatures less than approximately 1400°F (760°C). The gage can be used at higher temperatures by correcting for apparent strain if the ceramic adhesive continues to perform adequately.

E. Effects of Cryogenic Temperatures [68–70]

Strain can be measured with electrical-resistance strain gages to liquid-nitrogen temperatures (−320°F or −196°C) and below. Two factors must be carefully accounted for in using strain gages at this temperature extreme. The first effect is the change in gage factor with temperature, illustrated in Fig. 6.33. These results

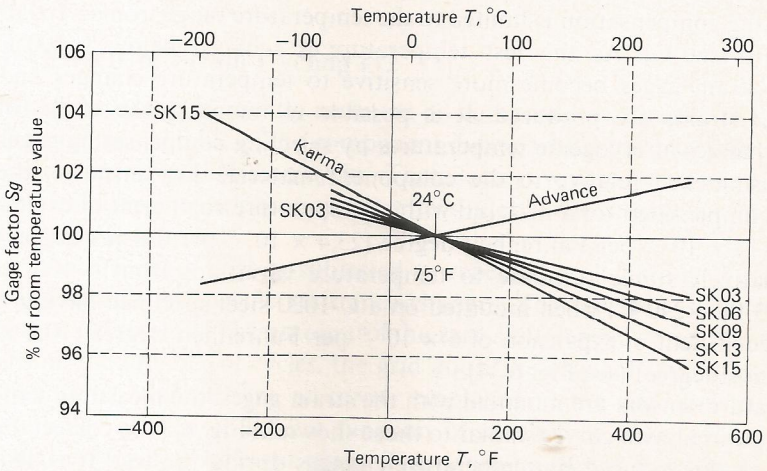

Figure 6.33 Changes in gage factor with temperature (from data by Telinde).

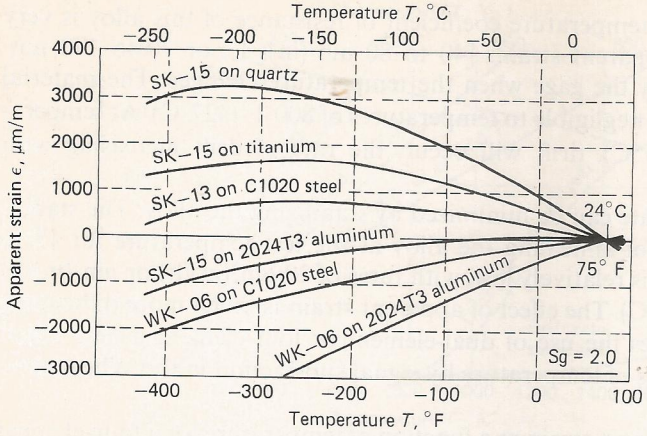

Figure 6.34 Apparent strain as a function of temperature for several selected-melt Karma alloys on different materials (from data by Telinde).

indicate that this correction is small, being only −1.8 and +3.8 percent, respectively, for Advance and the selected-melt Karma alloy SK-15 at −320°F (−196°C).

The second effect, which is extremely important to account for when measuring strains at cryogenic temperatures, is the very large apparent strains introduced by small changes in temperature. Karma alloys are preferred to Advance alloys because of their better stability at the temperature extremes, as shown in Figs. 6.15 and 6.16. Temperature-induced apparent strains for Karma strain gages mounted on a variety of materials are shown in Fig. 6.34.

Although both Advance and Karma strain gages are temperature-compensated, the compensation is limited to the temperature range from −100 to 500°F (−73 to 260°C). As the test temperature is reduced below −100°F (−73°C), the strain gages become more sensitive to temperature changes and large apparent strains are produced. It is possible to minimize the effects of temperature changes at cryogenic temperatures by selecting compensating gages which are mismatched relative to the component material. For instance, the Karma gage compensated for a material with a temperature coefficient of expansion equal to 13×10^{-6} per Fahrenheit degree (23.4×10^{-6} per Celsius degree) exhibits a relatively stable response to temperature variations from —100 to −400°F (−73 to −240°C) when mounted on a C-1020 steel specimen having a temperature coefficient of expansion of 6×10^{-6} per Fahrenheit degree (10.8×10^{-6} per Celsius degree) (see Fig. 6.34).

If temperature sensors are mounted with the strain gages, the measured temperatures can be used with curves similar to those shown in Fig. 6.34 to correct for the apparent strains induced by temperature changes during the test. It is also possible to use a four-element gage which is wired so that signal cancellation in

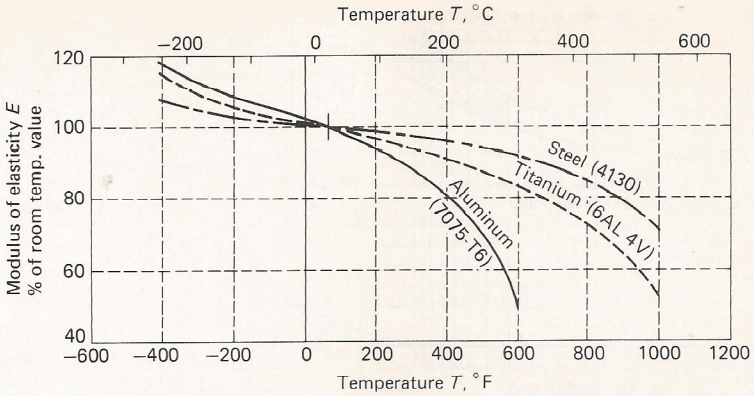

Figure 6.35 Change in elastic modulus as a function of temperature (from data by Telinde).

the Wheatstone bridge compensates for the temperature-induced response of the strain gages.

Cryogenic temperatures are usually obtained in tests by using liquid nitrogen, liquid hydrogen, or liquid helium. All three are excellent insulating materials, and it is not necessary or advisable to use electrical insulating compounds between the gage grid and the cryogenic fluid. The gage should be coated with a silicone grease to provide a heat shield and to eliminate the possibility of boiling of the liquid over the gage grid during the test.

Special consideration must also be given to changes in the mechanical properties of component materials at cryogenic temperatures. The effect of cryogenic temperatures is to increase the elastic modulus from 5 to 20 percent, as indicated in Fig. 6.35. The higher values of the elastic modulus must be employed in the stress-strain equations when converting the strain data to stress.

F. Effects of Strain Cycling [72–73]

Strain gages are frequently mounted on components subjected to fatigue or cyclic loading, and the life of the component during which the gage must be monitored can exceed several million cycles. Three factors which must be considered for this particular type of application are zero shift, change in gage factor, and failure of the gage in fatigue.

As the strain gage is subjected to repeated cyclic strain, the gage gridwork hardens and its specific resistance changes. The specific resistance change produces a zero shift. The amount of the zero shift depends on the magnitude of the strain, the number of cycles, the grid alloy, the original state of cold work of the grid alloy, and the type of carrier employed in the gage construction. Typical examples of zero shift as a function of number of strain cycles are shown in Fig. 6.36 for four different gages. The poorest gage for this type of application is the open-faced Advance grid (EA) gage, which begins to exhibit noticeable zero

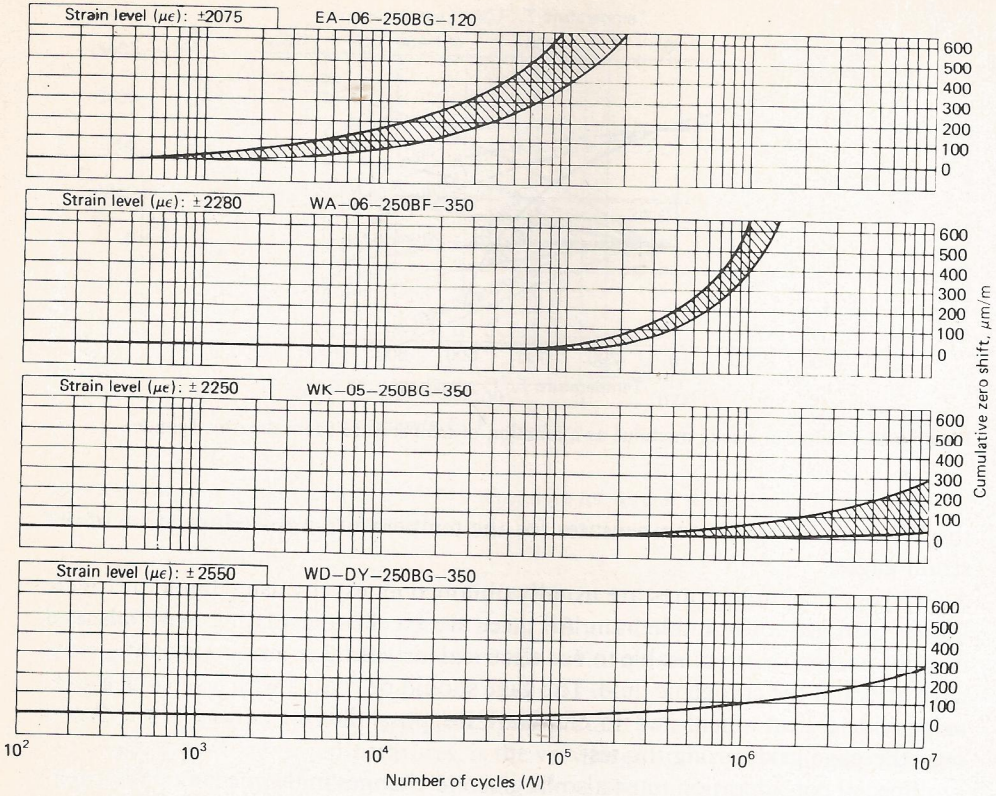

Figure 6.36 Zero shift as a function of fatigue exposure. (*Micro-Measurements.*)

shift at 10^3 cycles. Encapsulating the grid in a glass-reinforced epoxy-phenolic resin (WA type) improves the life, and exposures of 10^5 cycles at ± 2100 μin/in (μm/m) occur before zero shift becomes apparent. Further improvement can be achieved by using Karma (K) or isoelastic (D) alloys fully encapsulated in the glass-reinforced epoxy-phenolic carrier material with factory-installed lead wires.

The changes in gage factor are quite small due to strain cycling and in general can be neglected if the zero shift is less than a few hundred microinches per inch or micrometers per meter.

A very important factor to consider when using strain gages under fatigue conditions is the increase in sensitivity which occurs once a fatigue crack develops in the grid of the gage. The crack will usually develop in the grid near the lead wire on the tab. The presence of the crack produces a small increase in the resistance of the gage, which is monitored as an apparent strain. Thus the apparent gage factor has increased with the development and subsequent propagation of the fatigue crack.

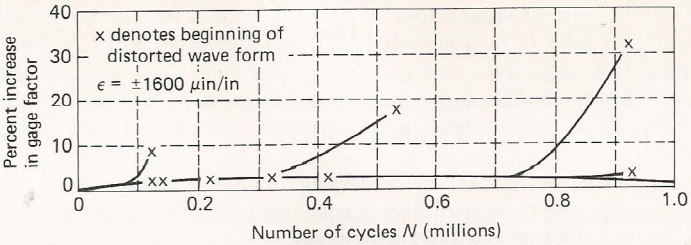

Figure 6.37 Increase in gage factor as a function of fatigue exposure for an annealed Advance foil gage. (*Micro-Measurements.*)

Typical results showing this increase in gage factor are shown in Fig. 6.37. It is important to note that the gage factor increased from 10 to 32 percent for the three gages which failed in fatigue. Also, the error in "calibration" existed over an appreciable fraction of the life of the gage.

EXERCISES

6.1 The strain sensitivity of most metallic alloys is about 2.0. What portion of this sensitivity is due to dimension changes in the conductor? What portion is due to changes in the number of free electrons and their mobility?

6.2 Advance or Constantan alloy exhibits a linear response of $\Delta R/R$ to strain ϵ for strains as large as 8 percent. Discuss why this is a remarkably large range of linearity with respect to strain when the elastic limit of the material may be as low as 21,000 lb/in^2 (145 MPa) and the modulus of elasticity is 22×10^6 lb/in^2 (152 GPa). Base the discussion on Eq. (6.2) and recall that Poisson's ratio for the material will increase from 0.3 to 0.5 as the material transforms from the elastic to the plastic state.

6.3 Describe the advantages and disadvantages of a strain gage fabricated using an isoelastic alloy.

6.4 Give several reasons why the foil strain gage is preferred over the bonded-wire strain gage.

6.5 List four different carrier materials used in strain-gage construction and give the reasons for their use.

6.6 Briefly discuss the conditions which would dictate using the following cements in a strain-gage installation:

(*a*) Cellulose nitrate cement (*b*) Epoxy cement
(*c*) Cyanoacrylate cement (*d*) NBS-x-142 ceramic cement

6.7 Describe two procedures used to evaluate the completeness of the cure of an adhesive being used to bond a strain gage to a specimen.

6.8 Determine the transverse sensitivity factor for a strain gage fabricated using Constantan alloy with $S_A = 2.11$ if it has been calibrated and found to exhibit a gage factor $S_g = 2.04$.

6.9 The transverse sensitivity factor K_t for a new grid configuration must be determined. It has been suggested that a simple tension specimen can be used with gages oriented in the axial and transverse directions to make the determination. Develop an expression for K_t in terms of Poisson's ratio of the specimen material and the ratio of the outputs from the two strain gages.